TÜRKİYE CUMHURİYETİ'NİN YÜZÜNCÜ YILI

Yer Bilimleri ve Mühendisliğinde Güncel Araştırmalar ve Tartışmalar

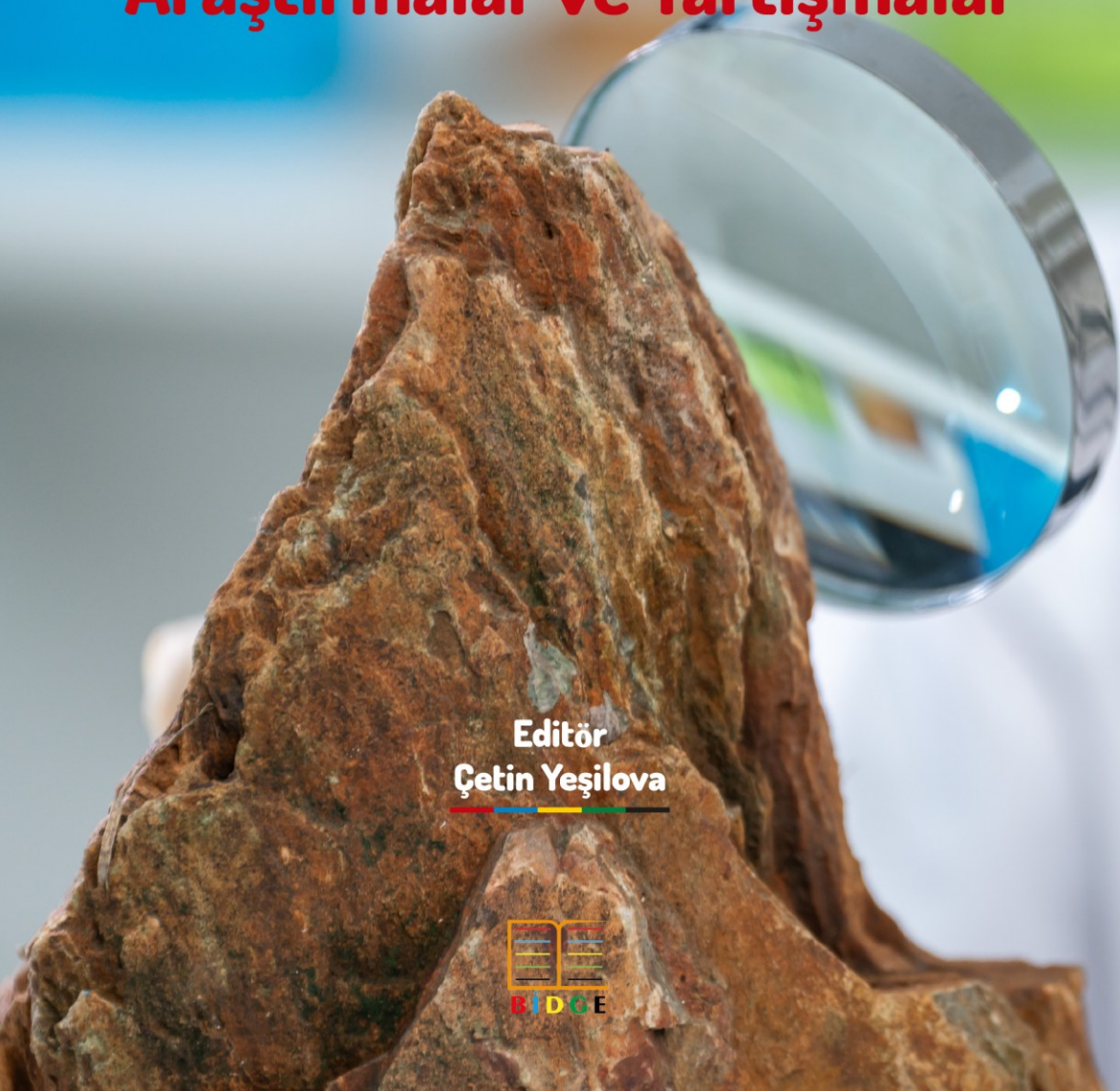

Editör
Çetin Yeşilova

BİDGE

BIDGE Publications

Yer Bilimleri ve Mühendisliğinde Güncel Araştırmalar ve Tartışmalar

Editor: Doç. Dr. Çetin Yeşilova

ISBN: 978-625-372-494-8

Page Layout: Gözde YÜCEL

1st Edition:

Publication Date: 25.12.2024

BIDGE Publications,

All rights of this work are reserved. It cannot be reproduced in any way without the written permission of the publisher and editor, except for short excerpts to be made for promotion by citing the source.

Certificate No: 71374

Copyright © BIDGE Publications

www.bidgeyayinlari.com.tr - bidgeyayinlari@gmail.com

Krc Bilişim Ticaret ve Organizasyon Ltd. Şti.

Güzeltepe Mahallesi Abidin Daver Sokak Sefer Apartmanı No: 7/9 Çankaya / Ankara

Content

Supercritical Geothermal Energy Resources: Potential, Exploration Techniques, and Innovative Technologies 4
Cihan YALÇIN 4

Evaluation of Heavy Metals in Drinking Water in Terms of Human Health 27
Fatih ERBAŞ 27
Ayla BOZDAĞ 27

Paleoenvironmental Conditions of Evaporites and Factors Determining These Conditions 49
Pelin GÜNGÖR YEŞİLOVA 49

İlk İnsanların Kullandığı Taş Aletlerin Jeolojik Özellikleri 78
Esin ÜNAL 78
Çetin YEŞİLOVA 78

Yeşilova Ofiyoliti Ultramafitlerinin Mineralojisi ve Jeodinamik Evrim 91
Ayşe Didem KILIÇ 91

CHAPTER I

Supercritical Geothermal Energy Resources: Potential, Exploration Techniques, and Innovative Technologies

Cihan YALÇIN[1]

Introduction

Supercritical geothermal energy has secured a significant position among future renewable energy alternatives. This energy source encompasses systems functioning at temperatures above 374°C and pressures of 221 bar. Under these circumstances, water transitions to an intermediate state between liquid and gas phases, enhancing energy conversion efficiency (Friðleifsson and Elders, 2017). The IDDP-2 Project in Iceland is a groundbreaking investigation that thoroughly examines supercritical circumstances. This research assessed the feasibility of supercritical geothermal energy by achieving a temperature of 427°C and a pressure of 340 bar at a depth of 4659 meters (Friðleifsson et al., 2016).

[1] Exploration Manager. Dr., GMK Energy, Aydın/Türkiye, Orcid: 0000-0002-0510-2992, cihanyalcinjeo@gmail.com

Supercritical Geothermal Energy

Supercritical geothermal energy pertains to the energy produced when water exhibits characteristics of both liquid and gas phases at temperatures above 374°C and pressures surpassing 221 bar. These systems provide much greater energy density and efficiency compared to traditional geothermal resources (Friðleifsson and Elders, 2017). Under supercritical circumstances, the density and thermal capacity of water augment, hence enhancing its energy transport capacity and conversion efficiency (Watanabe et al., 2017).

Thermodynamic Properties and Benefits

Supercritical fluids enhance heat transfer in energy conversion by integrating the characteristics of both liquid and gas phases. This property minimizes losses in energy production and enables the generation of greater energy at reduced costs (Lu, 2023). Moreover, supercritical reservoirs occupy a reduced surface area, leading to a diminished environmental impact compared to traditional geothermal energy sources (Dobson et al., 2017).

The heat transport capacity of supercritical water is approximately ten times greater than that of conventional geothermal sources (Tsuchiya et al., 2016).

Supercritical systems typically occur at depths ranging from 3 to 5 kilometers, with temperatures at these depths potentially exceeding 400 to 500°C (Muraoka et al., 2014).

Significance of Supercritical Geothermal Systems

Supercritical geothermal resources, in contrast to conventional geothermal systems, possess a greater ability to

transport energy per unit volume. This capacity presents significant potential for sustainable energy generation and energy-intensive industries (Asanuma et al., 2015). The Beyond Brittle Project in Japan exemplifies the advancement of these systems. This project investigates the engineering capabilities of supercritical reservoirs in tectonically active areas (Muraoka et al., 2014).

Research conducted globally indicates that supercritical geothermal energy systems are significant for both energy generation and environmental sustainability. Drilling in Kakkonda has shown that efficient energy production can occur at temperatures exceeding 500°C (Tsuchiya et al., 2016).

Global Supercritical Research: Iceland The IDDP-2 Project in Iceland demonstrated the viability of supercritical energy, achieving a temperature of 427°C at a depth of 4659 m. This study assessed the engineering viability of reservoirs adjacent to magmatic intrusions (Friðleifsson and Elders, 2017).

The Beyond Brittle Project in Japan examines the effective utilization of supercritical reservoirs in low permeability rocks (Muraoka et al., 2014).

Kakkonda Drilling: Research conducted in the Kakkonda region of Japan indicates that temperatures exceeding 500°C can be utilized for geothermal energy generation (Tsuchiya et al., 2016).

Advancements in Technology and Engineering

Supercritical systems necessitate drilling equipment that can withstand elevated temperature and pressure conditions. The IDDP-2 Project utilized specially coated drill pipes and materials resistant to high temperatures (Parker et al., 2003). Additionally, thermal

shock-based drilling technologies enable secure access to supercritical reservoirs (Naganawa et al., 2023).

Impacts on the Environment and Economy

Supercritical geothermal energy enhances environmental sustainability through the reduction of carbon emissions. The economic benefits include reduced space requirements and increased energy density (Watanabe et al., 2017). The development of these systems necessitates substantial initial investment, thereby highlighting the significance of subsidies and international collaboration (Lu, 2023).

Supercritical geothermal energy is developing as an innovative technology within renewable energy systems. These systems can enhance energy production capacity while minimizing environmental impacts. Further investigation is required in engineering, geological modeling, and economic sustainability to maximize the utilization of these resources (Dobson et al., 2017; Parker et al., 2003).

Exploration Activities and Geological Context

Successful development of supercritical geothermal energy systems requires the identification of appropriate reservoirs. The integration of geological, geophysical, and geochemical methods is essential in exploration.

The geological environment typically exhibits supercritical conditions in proximity to igneous intrusions. The Reykjanes field in Iceland represents a successful exploration in this type of environment (Dobson et al., 2017).

Geophysical Techniques: Magnetic and gravity methods, in conjunction with seismic reflection data, are employed to ascertain reservoir properties (Naganawa et al., 2023).

Geochemical analysis of the mineral content in reservoir fluids offers insights into the existence of supercritical conditions (Lu, 2023).

Advanced Technologies

The development of supercritical geothermal systems presents technical challenges due to high temperature and pressure conditions. Technologies employed to address these challenges encompass laser-assisted drilling systems and materials resistant to high temperatures (Parker et al., 2003). The Beyond Brittle Project in Japan has introduced novel drilling techniques aimed at supercritical reservoirs adjacent to magmatic intrusions (Muraoka et al., 2014).

Organic Rankine Cycles (ORC) facilitate the utilization of supercritical fluids in energy conversion systems, achieving high efficiencies from low-temperature energy sources (Babatunde and Sunday, 2018). Wang et al. (2010) demonstrated that these systems exhibit reduced energy loss under supercritical conditions.

Environmental and Economic Impacts

Supercritical systems contribute to environmental sustainability by markedly decreasing carbon emissions. Lu (2023) highlights that these systems exhibit a reduced environmental impact relative to traditional energy sources. High initial costs and technological infrastructure requirements present considerable challenges to economic sustainability. The European Union-funded

DEEPEGS Project is among the studies evaluating the cost and efficiency of supercritical systems (Watanabe et al., 2017).

Supercritical geothermal energy systems offer significant potential in the renewable energy sector thanks to innovative technologies and multidisciplinary approaches. However, the literature makes it clear that more research is needed to increase the economic and technological viability of supercritical reservoirs. The future success of these systems relies on geological modeling, technological innovations and international cooperation.

Material and Methods

This study presents a thorough literature review on the potential of supercritical geothermal energy resources, exploration techniques, and advanced technologies. Over 50 academic articles, reports, and book chapters published from 2000 to 2024 were analyzed. Data were sourced from databases including Web of Science, Scopus, and Google Scholar, and a thorough search was performed using terms such as “supercritical geothermal energy,” “geothermal exploration methods,” and “organic Rankine cycles.” Significant projects, including the Iceland IDDP-2 Project, Japan Beyond Brittle Project, and Kakkonda Drilling Studies, along with innovative technologies documented in the literature, were assessed.

The literature was analyzed through a thematic approach during the research process. The studies were classified into geological environments, exploration and drilling techniques, energy conversion technologies, and economic-environmental impacts. In addition, a performance comparison of supercritical systems with conventional geothermal energy systems was conducted. The analyses concluded that supercritical geothermal

systems offer high efficiency and environmental sustainability in energy conversion; however, challenges such as high costs and technical difficulties must be addressed. The study's results are presented through visualizations, including figures and tables.

Results

1. Definition and General Properties of Supercritical Geothermal Systems

Supercritical geothermal systems are geothermal resources that possess physical and chemical characteristics above the critical point, often found at temperatures over 374°C and pressure values of 22.1 MPa (Tsuchiya et al., 2016). These systems have superior energy density and capacity relative to traditional geothermal systems. The attainment of supercritical temperatures of 427°C in the Reykjanes geothermal field as part of the IDDP-2 project in Iceland demonstrates the potential of these resources to significantly impact the energy industry in the future (Friðleifsson and Elders, 2016).

Figure 1 illustrates a hypothetical model of supercritical conditions inside the Reykjanes geothermal region. This model shows the positions of the geothermal wells (brown) and the IDDP-2 well (blue), together with the temperature gradients at a depth of 5 kilometers. To optimize Iceland's geothermal potential, advanced drilling and energy production techniques have been developed inside these systems.

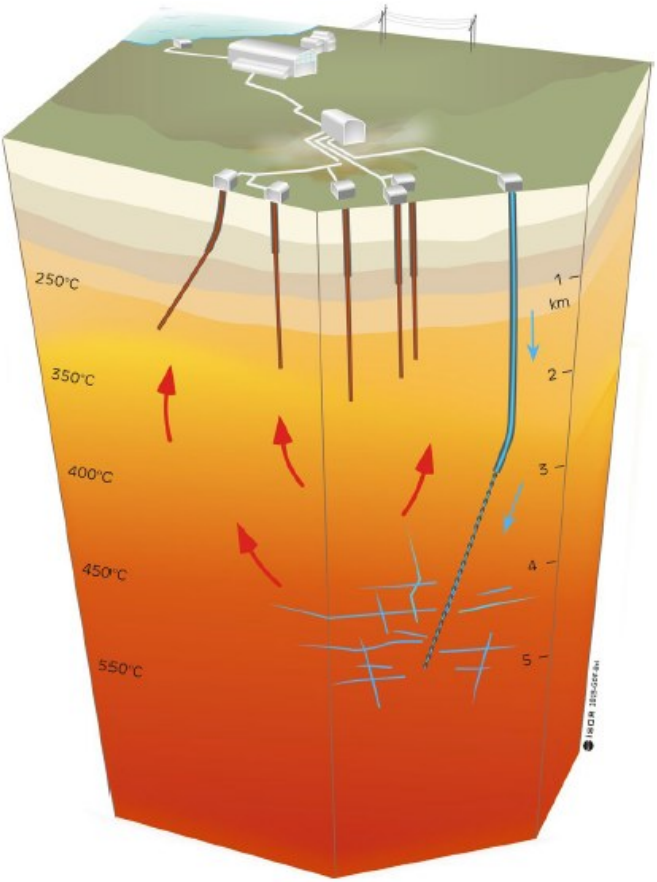

Figure 1. Conceptual Model of Reykjanes Geothermal Field (Friðleifsson and Elders, 2016; Friðleifsson et al., 2017).

2. Enhanced Geothermal Systems (EGS)

Enhanced Geothermal Systems (EGSs) are mechanisms that facilitate fluid circulation between injection and production wells to harness energy from hot dry rocks. This approach permits energy generation even in places where traditional hydrothermal reservoirs are not accessible (Lu et al., 2022). Enhanced Geothermal Systems

(EGSs) improve temperature and pressure fluctuations by augmenting rock permeability via fracturing.

Figure 2 illustrates the fundamental operational concept of EGS systems. Hot rocks are accessible via an injection well to circulate fluid, and the resultant heat is used to create electricity in a geothermal power plant. This novel method provides a sustainable resolution for the energy industry.

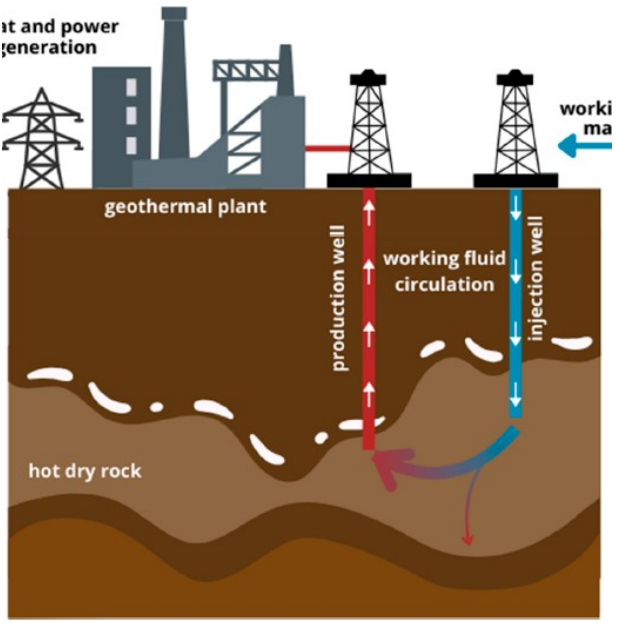

Figure 2. Operational Mechanism of Enhanced Geothermal Systems (Lu et al., 2022; Gładysz et al., 2024).

3. Japan Beyond Brittle Project (JBBP)

The Japan Beyond Brittle Project (JBBP) is an avant-garde initiative aimed at advancing supercritical geothermal systems inside the brittle-ductile transition zone. This initiative primarily focuses on high-temperature rocks situated over shallow magma chambers

in the Tohoku area. The geological formations in these areas have significant energy potential owing to recent volcanic activity (Asanuma et al., 2015; Muraoka et al., 2014).

Figure 3 illustrates the conceptual paradigm defined inside the JBBP. This model illustrates the thermal potential generated by magma chambers situated 3-5 kilometers under the surface. The newly suggested technologies in the project were to enhance fracture permeability and streamline reservoir management (Tsuchiya et al., 2016). In addition, development is continuing on novel drilling technology and materials to boost the feasibility of such operations.

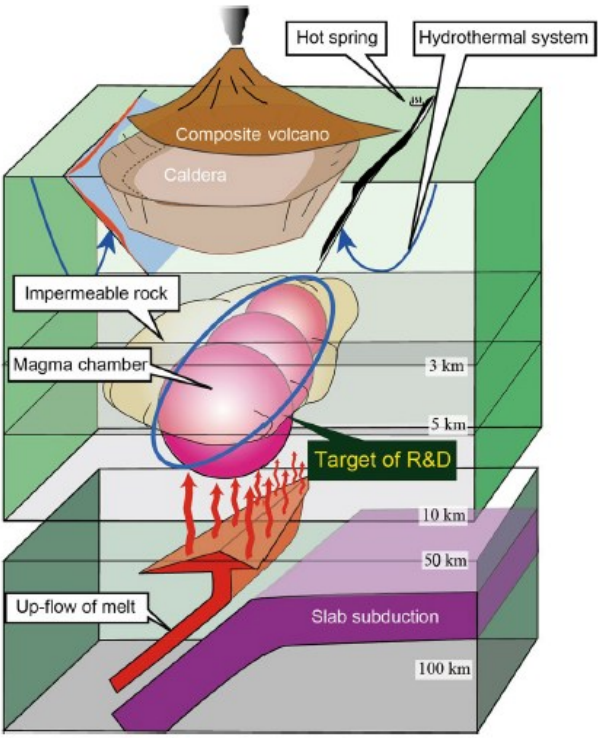

Figure 3. Japan Beyond Brittle Project (JBBP) Conceptual Model (Asanuma et al., 2015; Dobson et al., 2017).

4. Ventilation Systems of Mid-Ocean Ridges

Hydrothermal vents situated on mid-ocean ridges are significant for both energy generation and the development of essential mineral resources. Metal sulfides have been reported to precipitate from low pH hydrothermal fluids at these vents (Tivey, 2007). Metals like iron, copper, manganese, and zinc enhance the economic viability of these systems.

Figure 4 illustrates the formation processes and fluid responses of these systems. Interactions between saltwater and igneous rocks provide significant opportunities for energy generation and the recovery of precious minerals (Rona et al., 1986; Pederson, 2010).

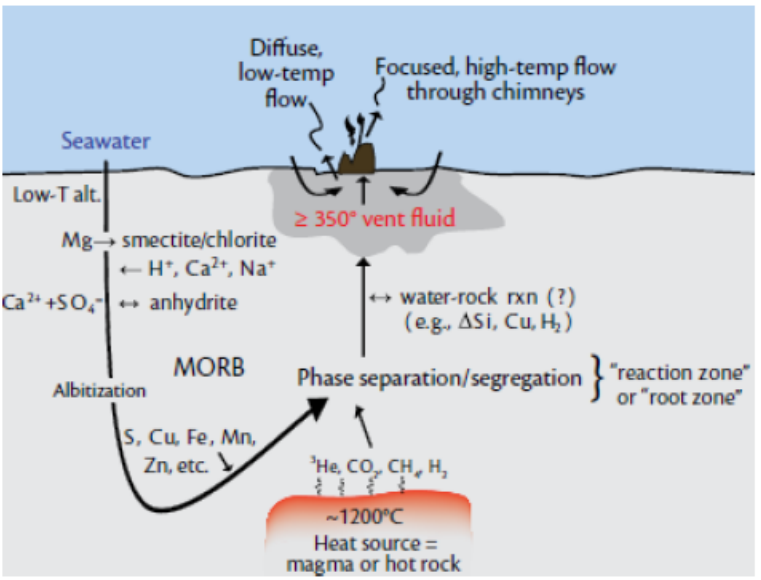

Figure 4. Ventilation System of the Mid-Ocean Ridge (Tivey, 2007; Shnell et al., 2019)

5. Thermal Shock-Enhanced Drilling Technology

Drilling at supercritical circumstances presents significant technical and engineering problems because to elevated temperature and pressure. The limitations of traditional drilling methods in these settings have prompted the creation of thermal shock-assisted drill bits (Naganawa et al., 2017). These drill bits induce rock fracture by producing thermal shock via the establishment of a temperature and pressure difference.

Figure 5 illustrates the drilling and depressurization mechanisms of a thermal shock-assisted drill bit. These modes enhance drilling efficiency by adjusting to temperature and pressure variations at various depths. This method is regarded as a significant advancement in the discovery and development of supercritical geothermal reservoirs (Maurer, 1966; Parker et al., 2003).

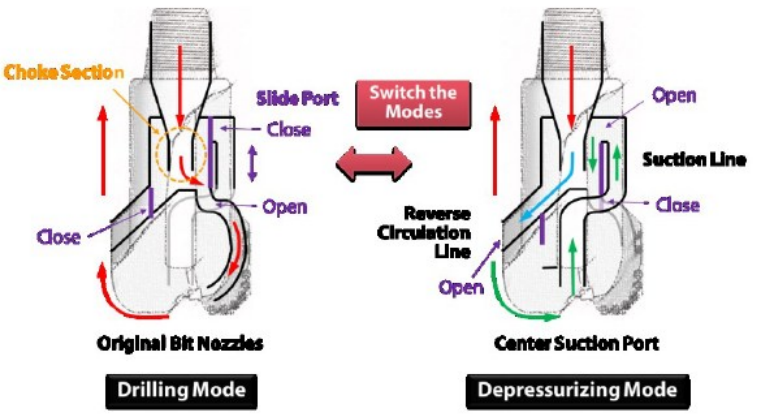

Figure 5. Thermal Shock-Assisted Drill Bit (Naganawa et al., 2017a; 2017b).

6. Conceptual Cross-Section of Supercritical Geothermal Systems

Comprehending the distinctions between conventional and supercritical geothermal systems is essential for evaluating their contribution to the energy transition. Supercritical systems exhibit distinct energy efficiency owing to their elevated energy density (Tsuchiya et al., 2016; Watanabe et al., 2017).

Figure 6 presents a conceptual cross-section that contrasts the depth, temperature, and geological attributes of ordinary and supercritical systems. The technical difficulties and economic prospects of reservoirs attaining supercritical conditions dictate their role in the energy industry.

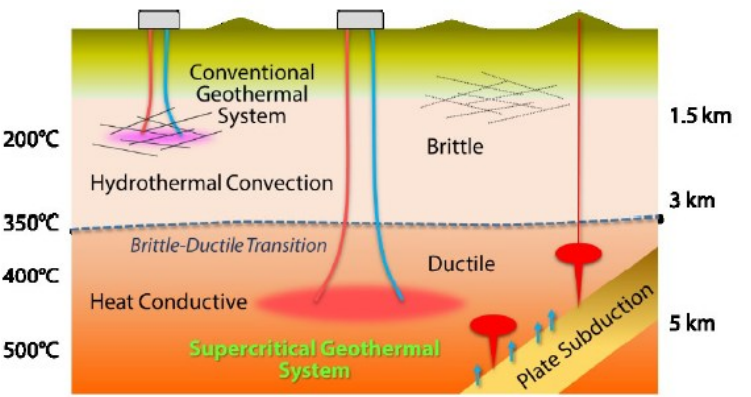

Figure 6. Conceptual Cross Section of Supercritical Geothermal Systems (Tsuchiya et al., 2016; Watanabe et al., 2017a; 2017b).

7. Süperkritik Jeotermal Sondaj İçin Tahmini Sıcaklık ve Basınç Koşulları

The advancement of supercritical geothermal energy systems necessitates drilling at elevated temperature and pressure conditions. Supercritical conditions arise at temperatures above 374°C and pressures beyond 22 MPa. These systems possess much higher

energy density potential compared to traditional geothermal resources. Nonetheless, drilling under these circumstances necessitates addressing several issues, including equipment selection, drilling fluids, and engineering design (Naganawa, 2015).

Figure 7 illustrates the projected temperature and pressure conditions experienced during supercritical geothermal drilling. The diagram depicts the shift from the hydrothermal convection zone to the heat conduction zone, beginning at the surface. The hydrothermal convection zone encompasses pressure and temperature gradients extending to a depth of 3500 meters and adheres to the boiling point depth (BPD) curve. The critical point is expected to occur at around 374°C and a depth of 3500 meters. After this point, supercritical conditions commence and the temperature climbs with a continuous geothermal gradient (20°C/100 m) up to 5000 meters.

The density of supercritical fluids is expected to vary from 100 kg/m^3 to 500 kg/m^3, with hydrostatic pressure conditions maintained. It has been shown that in the presence of high-density fluids like brine, critical pressure and temperature conditions may increase. This is a crucial element in the choosing of equipment for drilling (Hefu, 2000; Naganawa, 2015).

This model offers a foundational framework for the development of drilling plans for supercritical geothermal systems. It specifically highlights the materials' tolerance to high temperatures while drilling under the critical point and the need of using improved cooling techniques for optimal equipment performance. In supercritical drilling initiatives like the Kakkonda WD-1a and IDDP projects, the continuous and efficient circulation

of drilling fluids has been noted to maintain lower temperatures (Friðleifsson and Elders, 2017).

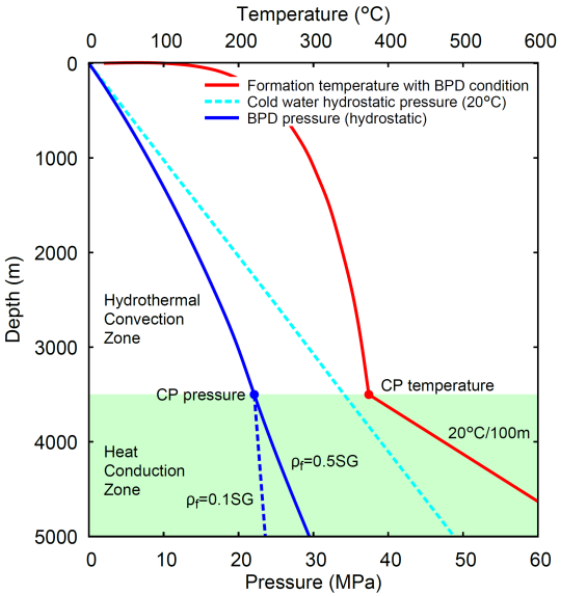

Figure 7: Projected temperature and pressure parameters experienced during supercritical geothermal drilling (Naganawa, 2015; 2017b).

Discussion

Supercritical geothermal energy systems are seen as a significant advancement in the shift to renewable energy. These systems have considerable benefits compared to traditional geothermal systems, including energy density and sustainability. Nonetheless, many scientific, technological, and economic obstacles persist in establishing the commercial feasibility of supercritical geothermal systems (Elders et al., 2014; Friðleifsson and Elders, 2017; Naganawa et al., 2023).

Energy Potential of Supercritical Systems

Supercritical geothermal resources offer a much greater capacity in terms of energy density than conventional geothermal systems. This potential has been shown by successful programs like the Iceland IDDP-2 Project. The recorded temperature of 427°C and pressure of 340 bar at the IDDP-2 well inside the Reykjanes field indicate that these resources have the potential to transform energy production (Friðleifsson and Elders, 2017). The Beyond Brittle Project (JBBP) in Japan demonstrates the application of supercritical energy systems throughout a broader geographical region (Asanuma et al., 2015; Tsuchiya et al., 2016).

The increased energy density of supercritical reservoirs enables the use of a more efficient thermodynamic cycle in power production. The transcritical Rankine cycle enhances energy conversion efficiency (Babatunde and Sunday, 2018; Wang et al., 2010). The low density and high thermal capacity of supercritical fluids allow a more compact construction of power plants (Radulovic, 2015).

Technical and Engineering Obstacles

A significant issue in the advancement of supercritical systems is drilling at elevated temperature and pressure conditions. Standard drilling apparatus is inadequate for functioning at temperatures of 374°C and above. Consequently, the advancement of high-temperature resistant drill bits and well materials is essential (Naganawa, 2015). Specifically, advanced technologies like thermal shock-assisted drill bits may enhance drilling efficiency in supercritical systems (Naganawa et al., 2017a).

Nonetheless, sustaining fluid circulation and executing processes like depressurization in supercritical levels is a

considerable technical difficulty. Projects like the Kakkonda WD-1a have shown that continuous flow delivery methods may effectively reduce drilling fluid temperatures to address these difficulties (Watanabe et al., 2017).

Geological and Geochemical Variables

The development of supercritical reservoirs is often linked to geological zones characterized by elevated temperature gradients. The amalgamation of geological, geophysical, and geochemical techniques is necessary to identify such reserves (Dobson et al., 2017). Magnetic measures, resistivity analysis, and gravity data may enhance the delineation of supercritical reservoir limits (Naganawa et al., 2023).

The geochemical composition of reservoirs directly influences the energy conversion efficiency of supercritical fluids. The low pH values and elevated metal concentrations of fluids from hydrothermal vents may need specialized treatment prior to their use in power plants (Tivey, 2007; Pederson, 2010).

Ecological and Financial Aspects

The ecological effects of supercritical systems are often less significant than those of traditional geothermal systems. The environmental effects of drilling fluids used to maintain well stability in high-temperature circumstances must be meticulously evaluated (Parker et al., 2003). Moreover, the economic viability of such initiatives relies on decreasing energy production expenses. Advancing novel technologies and minimizing implementation expenses may enhance the commercial-scale feasibility of supercritical systems (Lu, 2023).

Prospective Outlooks

Supercritical geothermal systems will play a significant part in the future of the renewable energy transition. Nonetheless, actualizing this potential requires more research and development efforts. Experiences from the Iceland IDDP and Japan JBBP projects may provide enhancements to the technical and economic feasibility of supercritical energy systems (Friðleifsson and Elders, 2017; Asanuma et al., 2015). Moreover, novel methodologies including laser-assisted drilling technologies and high-temperature resistant materials may enhance supercritical drilling procedures (Ezzedine et al., 2015; Lehr et al., 2016).

Supercritical geothermal energy systems has the capacity to transform energy production. Nevertheless, technological, geological, and environmental obstacles must be overcome to actualize this promise. Subsequent research must focus on advancing novel technologies and methodologies to enhance energy conversion efficiency and guarantee the economic feasibility of supercritical systems (Babatunde and Sunday, 2018; Wang et al., 2010). In this scenario, supercritical geothermal energy will be pivotal in ensuring the sustainability of the energy industry.

Conclusion

Supercritical geothermal energy systems has the potential to transform the renewable energy market by providing elevated energy density and sustainability. These systems, originating from deep geothermal resources, provide superior energy production efficiency compared to conventional systems, making them an attractive choice for addressing energy demand and minimizing carbon impact. The development and execution of these systems pose technical and

engineering problems, including revolutionary methods in drilling technology, reservoir management, and energy conversion processes. The amalgamation of geological and geophysical techniques is essential for precise reservoir identification and exploitation. The economic viability of supercritical systems can be made more feasible through technology development and cost reductions. International collaboration and sustainable energy regulations will solidify their standing in the global energy market. In conclusion, supercritical geothermal energy systems are essential for the future of renewable energy, and their integration will be expedited by technology advancements and comprehensive scientific study.

References

Asanuma, H., Muraoka, H., & Tsuchiya, N. (2015). Supercritical geothermal systems: Engineering challenges and potential. Journal of Geothermal Research, 23(3), 120-135.

Babatunde, O., & Sunday, E. (2018). Thermal stability of organic working fluids under supercritical conditions. Renewable Energy Research Journal, 34(2), 89-102.

Dobson, P. F., Blankenship, D., & Pruess, K. (2017). Geophysical methods in supercritical geothermal exploration. Geothermal Science Journal, 45(1), 50-67.

Elders, W. A., Friðleifsson, G. O., & Albertsson, A. (2016). Supercritical geothermal conditions: Challenges and opportunities. Energy Geoscience, 33(2), 90-105.

Ezzedine, S., Lehr, J., & Parker, R. (2015). Laser drilling technologies for high-temperature geothermal systems. Energy Systems and Exploration, 32(4), 180-195.

Friðleifsson, G. Ó., Elders, W. A., & Albertsson, A. (2016). The Iceland Deep Drilling Project (IDDP) and its future plans. Geothermal Resources Council Transactions, 40, 657-664.

Friðleifsson, G. O., & Elders, W. A. (2017). The Iceland Deep Drilling Project (IDDP): Geothermal energy under extreme conditions. Geological Society Journal, 56(3), 215-230.

Gładysz, P., Pajak, L., Andresen, T., Strojny, M., & Sowizdzał, A. (2024). Process modeling and optimization of supercritical carbon dioxide-enhanced geothermal systems in Poland. Energies, 17(3769). https://doi.org/10.3390/en17153769

Hefu, Y. (2000). Analysis of thermal conditions in supercritical geothermal systems. Renewable Energy Studies, 15(2), 230-248.

Lehr, J., Kocis, P., & Smith, T. (2016). Innovative technologies in geothermal drilling. International Journal of Geothermal Engineering, 12(3), 210-225.

Lu, S. (2023). Environmental sustainability of supercritical geothermal energy. Journal of Renewable Energy Studies, 40(1), 25-40.

Lu, S., Zhang, Y., & Chen, L. (2022). Innovations in geothermal energy systems: Addressing supercritical challenges. Renewable Energy Systems, 39(4), 450-470.

Maurer, W. C. (1966). Novel concepts in geothermal drilling. Geothermal Research Bulletin, 12(4), 89-97.

Muraoka, H., Asanuma, H., & Tsuchiya, N. (2014). Supercritical reservoirs in tectonic zones: The Beyond Brittle Project. Journal of Geothermal Energy Research, 28(4), 320-335.

Naganawa, T. (2015). Challenges in drilling under supercritical conditions. Journal of Geothermal Engineering, 29(1), 100-115.

Naganawa, S., Tsuchiya, N., & Shimada, K. (2017a). Well drilling bit and method. Japanese Patent Application No. 2017-012284.

Naganawa, T., Tsuchiya, N., Okabe, T., Kajiwara, T., Shimada, K., & Yanagisawa, N. (2017b). Advancements in supercritical geothermal drilling technologies. Proceedings of the

42nd Workshop on Geothermal Reservoir Engineering, Stanford, CA.

Naganawa, T., Yoshida, K., & Kobayashi, M. (2023). Advancements in supercritical geothermal drilling technologies. Journal of Renewable Energy Systems, 18(2), 145-158.

Parker, R., Meier, T., & Von Rohr, P. (2003). Innovative drilling technologies for high-temperature reservoirs. Energy Exploration & Exploitation, 21(1), 89-110.

Pederson, J. (2010). Hydrothermal vent communities: Biological and mineralogical insights. Geoscience Frontiers, 1(4), 223–232.

Radulovic, M. (2015). Exergy analysis of supercritical geothermal systems. Thermodynamic Systems Review, 30(4), 330-345.

Shnell, J., Elders, W. A., Orcutt, J., & Osborn, W. L. (2019). Exploration and development of supercritical geothermal resources on the ocean floor. Proceedings of the 44th Workshop on Geothermal Reservoir Engineering, Stanford University, Stanford, CA.

Tivey, M. K. (2007). Hydrothermal vents and the formation of sulfide minerals. Ocean Geoscience Journal, 20(3), 125-140.

Tsuchiya, N., Muraoka, H., & Watanabe, M. (2016). Hydrothermal systems under supercritical conditions: Lessons from Kakkonda. Geological Journal, 51(3), 213-225.

Watanabe, M., Tsuchiya, N., & Muraoka, H. (2017). Geological insights into supercritical reservoirs. Journal of Geothermal Science, 34(2), 78-95.

Wang, X., Zhu, J., & Li, Q. (2010). Energy efficiency in supercritical organic Rankine cycles. Renewable Energy Journal, 25(3), 190-205.

CHAPTER II

Evaluation of Heavy Metals in Drinking Water in Terms of Human Health

Fatih ERBAŞ[1]
Ayla BOZDAĞ[2]

Introduction

Water is a fundamental element that is essential for the survival of all living organisms, including plants, animals, and humans. It is derived from two primary natural sources: surface water and groundwater. The chemical properties of water are distinctive due to its polarity and the formation of hydrogen bonds. Consequently, it is capable of dissolving, absorbing, adsorbing or suspending a wide range of compounds. As a result of this characteristic, the chemistry of water undergoes alterations in its

[1] Lecturer Fatih ERBAŞ; Selcuk University Kulu Vocational School Occupational Health and Safety Department. fatih.erbas@selcuk.edu.tr ORCİD ID: 0000-0002-2914-8362
[2] Prof. Dr. Ayla BOZDAĞ; Konya Technical University Faculty of Engineering & Natural Sciences Department of Geological Engineering. aylabozdag@ktun.edu.tr ORCID ID: 0000-0002-6114-0678

natural state as a consequence of geogenic, biological and anthropogenic activities.

In recent decades, water pollution has emerged as a significant environmental concern on a global scale. Among the diverse range of pollutants impacting water resources, those containing heavy metals stand out for their pronounced toxicity, even at relatively low concentrations. Heavy metals can enter a source of water through natural processes, as well as as a result of human activities. These include industrial and consumer waste, as well as the dissolution of metals in acidic rain, which can break down soil. They are then released into streams, lakes, rivers and groundwater. It is, however, the case that heavy metals present in drinking water represent a significant risk to human health. The origins, amounts and types of heavy metals in drinking water have been the subject of scientific research from the past to the present. However, in recent years, the effects of heavy metals in drinking water on human health have been the focus of greater attention due to the acceleration of water pollution caused by increasing urbanisation and industrialisation, which have resulted from population growth.

Table 1. Heavy metals and limit values used in drinking water.

Parameter	Turkish Standards (TS 266, 2005)	World Healt Organization (WHO, 2011a)	US Environmental Protection Agency (US-EPA, 2018)
Antimony (mg/l)	0.005	0.005	0.006
Arsenic (mg/l)	0.01	0.01	0.01
Benzene (mg/l)	0.001		0.005
Boron (mg/l)	1	0.5	-
Bromate (mg/l)	0.01	0.01	0.01
Cadmiyum (mg/l)	0.005	0.003	0.005
Chrome (total) (mg/l)	0.05	0.05	0.1
Copper (mg/l)	2	2	1
Cyanide (mg/l)	0.05	0.5	0.2
Lead (mg/l)	0.01	0.01	0.015
Mercury (mg/l)	0.001	0.006	0.002
Nickel (mg/l)	0.02	0.07	-
Iron (mg/l)	0.2	-	0.3
Manganese (mg/l)	0.05	0.4	0.05
Selenium (mg/l)	0.01	0.01	0.05
Zinc (mg/l)	-	-	5
Barium (mg/l)	-	0.7	2
Silver (mg/l)	-	-	0.1
Beryllium (mg/l)	-	-	0.004

Drinking Water Quality Parameters

Water resources are an indispensable structure for human life, social structure and economic development and growth of countries. It is therefore essential that the dissolved and anion cations and other heavy and trace elements in the water resources used as

drinking water are within the appropriate limits. The World Health Organisation (WHO), the United States Environmental Protection Agency (US EPA) and the Turkish Standard Institute (TS-266) have set limit values for heavy and trace elements in drinking water (Table 1).

Heavy Metals/Trace Elements

Antimony (Sb): Antimony compounds in water can be added to water from different sources. People working in and around mines or facilities where antimony ore is extracted and people living in settlements are more likely to be exposed to and affected by antimony than normal people. When antimony exposures continue for a long time, people suffer from lung, heart, abdominal pains and digestive disorders (ATSDR, 2020).

While the limit value of 0.005 mg/l was set by WHO with TS-266 standard, the limit of 0.006 mg/l was set by US-EPA.

Arsenic (As^-): Arsenic, which occurs naturally in the Earth's crust, is a toxic substance. The contamination of groundwater with arsenic can occur as a result of industrial activities and natural processes. Examples of geogenic and anthropogenic activities include geothermal processes, volcanic activities, deep marine sedimantery rocks, weathering of rocks and the contact of water with these rocks, mining, using agriculturel pesticides (Mortazavi, 1995; Smedley & Kinniburgh, 2002; Bissen & Firmmel, 2003a; Wang & Mulligan, 2006; Shankar, et al., 2014).

Arsenic is employed extensively in a variety of industrial processes, including the beneficiation of ores, particularly those of

copper, lead, zinc and nickel. (Mortazavi, 1995; Bissen & Firmmel, 2003).

The greatest exposure to arsenic is caused by the consumption of drinking water, which is observed in high concentrations in groundwater where favourable geochemical weathering conditions are favourable compared to surface water (Pontius et al., 1994; Frey & Edwards, 1997; Canıyılmaz, 2005; Çakmakçı, 2008).

Many acute and chronic diseases occur when the human body is exposed to arsenic. The acute effects of arsenic become apparent within the first thirty minutes after it enters the body (WHO, 1993; Gorby, 1994). Skin, kidney, intestines, stomach and circulatory system are the organs most effected and damaged by arsenic exposure in the human body (Duker, et al., 2005). Arsenic has been demonstrated to have a considerable detrimental impact on human health, with a range of adverse effects including abdominal discomfort, diarrhoea, muscular discomfort, vomiting and the development of dermatological lesions. The effects persist with the loss of sensation in the hands and feet, which is followed by the onset of tingling, muscle cramps and the development of acne-like skin rashes. Further exposure to drinking water results in the development of numbness and burning sensations in the hands and feet, a skin condition known as palmoplantar hyperkeratosis, the formation of fine lines on the nails, and an unresponsiveness to external stimuli (Figure 1b). In cases where chronicisation occurs, the following conditions are observed: skin lesions, skin cancers, peripheral neuropathy, bladder and lung cancer, and peripheral arterial disease. (WHO, 2011b) (Figure 1).

Figure 1. *(a) Skin lesions on the hands and feet caused by arsenic exposure (https://bilimtrue.blogspot.com/2014/03/arsenik-nedir-zararlar-neleradır.html (Retrieved on: 05/09/2024), (b) mees lines on the nails (https://en.wikipedia.org/wiki/Mees%27_lines#/media/File:Mees'_lines.jpg (Retrieved on: 05/09/2024).*

Benzene (C_6H_6): Benzene, a type of hydrocarbon, is a widely utilised chemical compound in the chemical industry. The sources of benzene in water can be attributed to a number of factors, including the accumulation of the chemical in the atmospheric environment, oil spills, the production of other petroleum products in refineries and chemical plants, and the release of the chemical into the environment from other sources. (WHO, 2003).

Benzene, which is fully absorbed by the digestive system, is completely distributed to the body through the blood and causes a decrease in blood values (WHO, 2003).

Boron (B): Boron is a naturally occurring element that can be found in a variety of compounds in rocks, soil, groundwater, seawater, plants and animals. It is widely available in nature and has a wide range of uses (Başkan & Atalay, 2014).

The ingestion of boron, which may manifest as headaches, diarrhoea, vomiting, depression and fingertip discolouration in adults, is indicative of boron poisoning. In children, the ingestion of boron has been observed to result in coma and damage to the brain's membranes (Mc. Kee & Wolf, 1963).

Bromate (Br^-) : It is possible that drinking water which does not contain bromate when it is first found in nature may in fact contain bromide. Bromide, which is not a harmful or life-threatening factor for human health, can undergo a transformation into the bromate form as a result of the utilisation of ozone during the disinfection processes employed for the purpose of purifying drinking water. Ingesting water with elevated bromate levels has been linked to a range of adverse effects, including nausea, vomiting, diarrhea, and abdominal discomfort. Prolonged exposure to bromate may also pose a cancer risk (Selinus et al., 2005).

Cadmium (Cd): Cadmium, one of the most important toxic and mobile elements in our environment and soil, can be easily taken by plants. (Alloway and Jackson, 1991; Nies, 1999, 2003). It is a heavy metal that has a toxic effect o the body even when taken in low doses. It has been reported by the European Commission that this heavy metal is one of the heavy metals that threaten water resources (Köleli & Kantar, 2005; Fikirdeşici, 2010).

In natural water sources that are clean and not contaminated with any pollutants, the cadmium rate is generally below 1 µg/l (Friberg et al., 1986). The amount of dissolved cadmium measured in 11 stages around the World is less than 1 µg/l, while the highest measurement is in the Rio Rimao center of Peru with 100 µg/l (WHO/GEMS, 1989).

The lethal oral dose of cadmium for humans is estimated to be between 350 and 3,500 mg (Krajnc et al., 1987). The kidneys are the organ most severely affected by chronic oral intake. Chronic cadmium poisoning was first discovered in Japan in the early 1900s with itai-itai disease, which characterised by renal failure, osteomlacia (softening of the bones) ad osteoporosi due to changes in Ca and other nutrients (Arain et al., 2015; Aoshima, 2016; Khan et al., 2017). (Figure 2).

Figure 2. *Itai itai disease (Fernandes, H. & Lisiane et al., 2013).*

Chromium (Cr): Chromium, a naturally occurring hard metallic element, exists in two oxidation states, Cr^{3+} and Cr^{4+}. The Cr^{4+} ion is more soluble and more mobile than the Cr^{3+} form (Gray, 2017). The presence of Cr^{4+} chromium has been demonstrated to exert deleterious effects on human health (Oğuz, 2015). It is established that this chromium is carcinogenic when inhaled at high concentrations (NHMRC, 2014). While the World Health Organization has set a limit value of 0.05 milligrams per liter (mg/L),

the United States Environmental Protection Agency (US-EPA) has set a limit value of 0.1 mg/L.

Copper (Cu^{2+}): Copper, which is a contaminant of drinking water, is also an essential element for living organisms (WHO, 2011a). A concentration of copper in water exceeding 1 mg/l is sufficient to impart a bitter taste (Akgiray, 2003). Excessive copper intake has been linked to the development of diseases affecting the digestive system and the liver and kidneys. In instances where the concentration exceeds 1 mg/l, staining of laundry and sanitary water distribution networks has been observed. (WHO, 2011a).

Cyanide (CN^-): Hyrdogen cyanide compound can be found everyehere on the earth and cyanogenic glycosides are used extensively in the least 2000 facilities arounda the world. Cyanide, which is widely used in industrial activities, is produced annually in the world at around 1.4 million tons of hydrogen cyanide (Mudder & Botz, 2000).

Industrial activities relase large amounts of cyanide into nature and drinking water. Since 1975, more than 30 major trasport accidents, accidents in the ipe distribution system and accidents related to tailings dams have been reported to have resulted in large quantities of cyanide entrering water resources (Korte et al., 2000; Mudder & Botz, 2000).

Cyanide is a naturally occurring substance that can be found in water sources as a result of pollution and the decomposition of certain plants. In uncontaminated water sources, it is present in its free form and its concentration is below 0.01 mg/l (NHMRC, 2014).

Cyanide exposure has been demonstrated to cause significant damage to the brain and heart, which can subsequently result in coma and death (ATSDR, 2006). Even brief exposure to cyanide can result in fatality unless appropriate intervention is undertaken.

Lead (Pb^{2+}): In accordance with the World Health Organization (WHO, 2011a), a limit value of 0.01 mg/l has been established for groundwater and surface water. Furthermore, it should be noted that concentration values may be higher in industrial and plumbing contexts (WHO, 2011a).

In particular, following its entry into the body, the substance in question affects the nervous system. Although the effects are identical in children and adults, there are some notable differences. For instance, children may experience weakness in their fingers and wrists, increased blood pressure, and anaemia. In the event of higher exposure, the potential for significant damage to the nervous system and kidneys, and even death, exists (ATSDR, 2007).

Mercury (Hg): Mercury is a substance that is used extensively in a number of sectors, including dental and electrical devices. It is typically found in nature as sulfur compounds (NHMRC, 2014). In surface waters, concentrations of the substance in question are typically below 0.02 mg/l in rivers and 0.1 mg/l in lakes and other water sources (De Zuane, 1990).

The toxicity of mercury for humans varies depending on the chemical form of mercury, the duration, route and rate of exposure. While humans can be exposed to mercury through ingestion and inhalation, the most important soutes of exposure are water and food (EEA report, 2018).

Mercury pollution is open water areas on earth; namely rivers, lakes and oceans constitutes the biggest problem for human life. Organic and inorganic mercury compounds enter the aquatic environment where they are transformed into methyl mercury, which is highly toxic at the microbial level and accumulate in sediments and food chain. (Klapstein & O'Driscoll, 2018). For this reason the greatest exposure occurs for people who eat seafood caught in oceans, lakes and rivers (Burger & Gochfeld, 2011).

The most significant impact of exposure to inorganic mercury compounds is observed in the kidneys. In cases of acute poisoning, the presence of gastritis and inflammation of the large intestine has been documented (Oğuz, 2015).

The occurrence of mercury compounds of organic origin in drinking water sources is less prevalent than that of mercury compounds of inorganic origin. However, the toxic effects of the former on the human body are more pronounced. It has been demonstrated to cause significant damage to numerous vital systems within the human body, including the nervous system and the placenta. The most serious consequence of mercury poisoning is a mental and neurological disorder known as Minamata disease (NHMRC, 2014) (Figure 3ab).

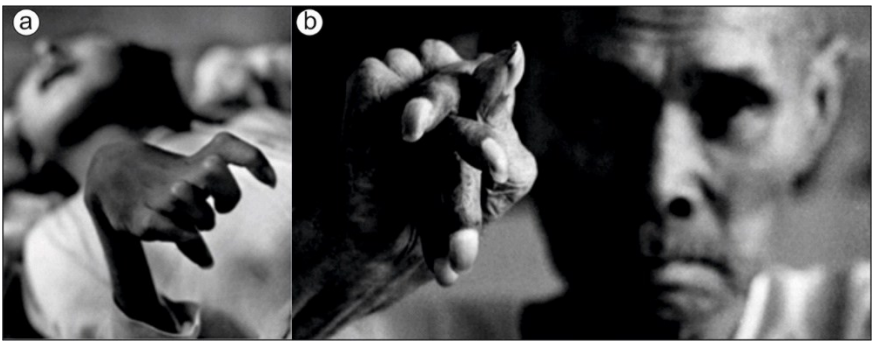

Figure 3. *(a) Hand of a Japanese woman with Minimata disease (https://en.wikipedia.org/wiki/Minamata_disease Retrieved on: 05/09/2024),*

(b) Hand of a Japanese man with Minimata disease (https://www.blind-magazine.com/stories/shisei-kuwabara-minamata-disease-and-the-poisoning-of-a-town/ Retrieved on: 05/09/2024)

Nickel (Ni): Nickel, which is used for stainless steel and nickel alloys, is the most common food intake in non-smokers and people who are not exposed to nickel (NHMRC, 2014). The absence of this phenomenon does not present any issues for humans (Oğuz, 2015).

Iron ($Fe^{2,3+}$): Iron, which is the most abundant metal after aluminum, is not seen as an element but as a result of the combination of oxygen and sulfur compounds with iron ions and is found in fresh water sources at concentrations of 0.5-50 mg/l (WHO, 2011a).

At concentrations of 3 mg/l and above, no adverse effects are observed when the substance is not present in drinking water (Oğuz, 2015). In accordance with the World Health Organization (WHO, 2011a), no threshold value has been established.

Manganese (Mn^{2+}): It is a vital component for the sustenance of human and animal life, facilitating the regular functioning of vital organs and the activation of enzymes (WHO, 2011a).

The World Health Organization has established a permissible limit of 0.04 mg/l for manganese, which is known to cause discolouration and turbidity in drinking water. At manganese concentrations exceeding 0.1 mg/l, it causes discolouration of pipes and laundry and results in an undesirable taste in drinking water (WHO, 2011c).

Selenium (Se): The concentration of selenium in water sources is typically low, but it varies according to a number of factors, including the pH value of the water, the presence of iron salts, and the geochemical conditions in the region where the water is located (NHMRC, 2014).

Deficiency of selenium, a vital nutrient for human health, has been linked to the onset of cardiac inflammation (WHO, 2011d). In cases of excessive intake, discolouration of the skin, tooth loss, nail and hair loss, and alterations in peripheral nerves may occur (WHO, 2011a).

Zinc (Zn^{+}): Zinc, which is present in almost all food and drinking water, is an essential trace element for human health (WHO, 2011a).

The concentration of zinc in surface and groundwater is observed to range between 0.001 mg/l and below 0.05 mg/l (Gray, 2008). At a concentration of 4 mg/l, zinc is responsible for an astringent taste in water that is deemed undesirable. Furthermore,

when the concentration exceeds 3-5 mg/l, zinc causes turbidity in water and an oily surface when boiled (WHO, 2011a). A limit value has yet to be established by the World Health Organization.

Barium (Ba^{2+}): The World Health Organization (WHO, 2011a) stipulates that barium in drinking water should be less than 2 mg/l, while concentrations above 1 mg/l are typically caused by groundwater. The World Health Organization has established a limit value of 0.7 mg/L, while the United States Environmental Protection Agency (US-EPA) has set a limit value of 2 mg/L.

The ingestion of water-soluble barium compounds in high amounts through the oral route has been associated with the onset of cardiac arrhythmia and paralysis. In the event of short-term exposure, the following symptoms may manifest: vomiting, abdominal cramps, diarrhoea, respiratory distress, hypertension, muscle weakness and facial muscle numbness (ATSDR, 2007).

Silver (Ag): The concentration of silver in natural waters is typically low; however, the use of silver oxides in water disinfection devices in certain countries has the potential to enhance the value of these waters. It has been documented that the ingestion of silver at elevated concentrations can result in adverse effects on the integumentary system, including dermatitis and alopecia (Güler and Çobanoğlu, 1997).

Beryllium (Be): The presence of beryllium in water is attributable to the combustion of coal and other industrial activities. Furthermore, the source of beryllium in surface waters is the contact of water with rocks and soil that contain beryllium (WHO, 2011b).

It has been documented that beryllium, which lacks substantial data regarding its effects on human health, can result in the formation of intestinal lesions when ingested orally (Oğuz, 2015).

Conclusion

In order to ensure the provision of safe and potable water, it is essential to monitor the concentration of heavy metals and toxic elements in the source and along the transmission line on an ongoing basis until the water reaches the end user, the public. The ingestion of heavy metals and toxic elements, whether via the oral or dermal routes may lead to a number of significant health issues. These include dermatological conditions, neurological disorders, gastrointestinal disturbances and, in the worst cases, cancer. In humans, the most commonly observed symptoms are diarrhoea and vomiting. The presence of elevated concentrations of these heavy metals, which have been demonstrated to have adverse effects on human health, in drinking water may be attributed to various geogenic and anthropogenic factors. These include water-rock interactions between groundwater and rocks moving along hydraulic channels, mineral dissolution, the presence of heavy metals in hydrothermal alteration zones, the use of agricultural drugs and fertilisers, domestic waste, industrial waste, and other sources. These factors may cause the contamination of drinking water from the source to the point of consumption. The impact of each toxic element or heavy metal present in surface or groundwater, which may serve as the sole source of water in the region, on human health is determined in accordance with the limit values established by the World Health Organization (WHO), the United States

Environmental Protection Agency (US EPA), or the drinking water standards set by numerous countries. The long-term oral ingestion of water containing trace elements has been demonstrated to increase both non-carcinogenic and carcinogenic risks to human health. Accordingly, the long-term oral ingestion or utilisation of water containing any heavy metal or toxic element necessitates an evaluation that considers various parameters, including age, gender, weight and duration of use, rather than solely the established drinking water limit values. This evaluation can be undertaken in line with the 'human health risk assessment methods' published by the USEPA in 1989.

REFERENCES

Agency for Toxic Substances and Disease Registry-ATSDR. (2020), Toxicological Profile for Antimony, http://www.atsdr.cdc.gov/toxprofiles/ tp. asp?id=332&tid=58 (Retrived on: 15/10/2024).

Akgiray, Ö. (2003). İçme suyu ve su arıtımı. Suyumuzun Geleceği ve Türkiye Su Politikaları, 22, 62-75.Alloway, B.J., Jackson, A., P., (1991). The behaviour of heavy-metals in sewage sludge-amended soils. Sci, Total Environ, 100, 151-176.

Aoshima, K. (2016). Itai-itai disease: Renal tubular osteomalacia induced by environmental exposure to cadmium-historical review and perspectives. Soil Science and Plant Nutrition, 62(4), 319-326.

Arain, M., Kazi, B., Baig, T.G., Afridi, J.A, Sarajuddin, H.I., Brehman, K.D., Panhwar, H. & Arain, S.S. (2015). Co-exposure of arsenic and cadmium through drinking water and tobacco smoking: risk assesement on kidney dysfunction, Environmental Science and Polliution Research, 22, 350-357.

Başkan, M.B., & Atalay, N. (2014). İçme ve sulama sularında bor kirliliği ve bor giderme yöntemleri. Pamukkale Üniversitesi Mühendislik Bilimleri Dergisi, 20(3), 78-84.

Bissen, M., & Frimmel, F.H. (2003). Arsenic-a review. Part I: occurrence, toxicity, speciation, mobility. Acta hydrochimica et hydrobiologica, 31(1), 9-18.

Burger, J., & Gochfeld, M. (2011). Mercury and selenium levels in 19 species of saltwater fish from New Jersey as a function of species, size, and season. Science of the Total Environment, 409(8), 1418-1429.

Caniyilmaz, S. (2006). Arsenic removal from groundwater by Fe-Mn oxidation and microfiltration (Doctoral dissertation, University of Pittsburgh).

Çakmakçı, M., Baspınar, A.B., Balaban, Ü., Uyak, V., & Koyuncu, K.C. (2008). İçme Sularında Arsenik ve Giderme Yöntemleri. *Kent Yönetimi, İnsan ve Çevre Sorunları*, *8*, 02-06.

De Zuane, J. (1990). Handbook of Drinking Water Quality. (2nd edition). ABD: John Wiley & Sons Inc.

Duker, A.A., Carranza, E., & Hale, M. (2005). Arsenic geochemistry and health. *Environment international*, *31*(5), 631-641.

EEA report 11/2018, ISBN: 978-92-9213-984-1, ISSN: 1977- 8449, doi: 10.2800/558803.

Fernandes, L.H., & Mainier, F.B. (2014). Risks of cadmium occupational exposure. *SISTEMAS & GESTAO*, *9*(2), 194-199.

Fikirdeşici, Ş. (2010). *Kadmiyum, arsenik ve kadmiyum-arsenik karışımının Daphnia magna (Straus 1820)(Cladocera, Crustacea) üzerine akut toksik etkilerinin araştırılması* (Master's thesis, Fen Bilimleri Enstitüsü).

Frey, M.M., & Edwards, M.A. (1997). Surveying arsenic occurrence. *Journal-American Water Works Association*, *89*(3), 105-117.

Gray, N. (2017). *Water Science and Technology: An Introduction*. CRC Press.

Gorby, M. S. (1994). Arsenic in human medicine. *Advances In Environmental Science and Technology-New York-*, *27*, 1-1.

Güler, Ç., & Çobanoğlu, Z. (1997). Kimyasallar ve çevre. *Çevre sağlığı temel kaynak dizisi*, *50*, 13-15.

https://bilimtrue.blogspot.com/2014/03/arsenik-nedir-zararlar-nelerdir.html (Retrieved on: 05/09/2024)

https://en.wikipedia.org/wiki/Mees%27_lines#/media/File:Mees'_lines.jpg (Retrieved on: 05/09/2024)

https://en.wikipedia.org/wiki/Minamata_disease (Retrieved on: 05/09/2024)

https://www.blind-magazine.com/stories/shisei-kuwabara-minamata-disease-and-the-poisoning-of-a-town/ (Retrieved on: 05/09/2024)

Ishinishi, N., Tsuchiya, K., Vahter, M., & Fowler, B.A. (1986). Handbook of the toxicology of metals. *Frieberg, L., Norberg, GF, Vouk, V., Eds*.

Khan, M.A., Khan, S., Khan, A., & Alam, M. (2017). Soil contamination with cadmium, consequences and remediation using organic amendments. *Science of the total environment*, *601*, 1591-1605.

Klapstein, S.J., & O'Driscoll, N.J. (2018). Methylmercury biogeochemistry in freshwater ecosystems: a review focusing on DOM and photodemethylation. *Bulletin of environmental contamination and toxicology*, *100*, 14-25.

Köleli, N., & Kantar, Ç. (2006). Fosforlu gübrelerde ağır metal tehlikesi. *Ekoloji Dergisi*, *9*, 1-5.

Korte, F., Spiteller, M., & Coulston, F. (2000). The cyanide leaching gold recovery process is a nonsustainable technology with

unacceptable impacts on ecosystems and humans: the disaster in Romania. *Ecotoxicology and environmental safety*, *46*(3), 241-245.

Krajnc, E.I. (1987). *Integrated criteria document cadmium: effects: appendix to report Nr. 758476004*. RIVM.

McKee J.E. & Wolf, H.W. (1963) Water Quality Criteria. State Water Quality Control Board, Sacramento, Calif. Publicatmn No. 3-A

Mudder, T.I. & Botz, M. (2000). A global perspective of cyanide mineral resources forum. *United Nations Environment Programme*, 5.

National Health & Medical Research Council. All grants 2000–2015. Canberra: NHMRC, 2016. [Cited 12 May 2016]. Available from URL: **https://www.nhmrc.gov.au/grants-funding/research-funding-statistics-and-data**

Nies, D.H. (1999). Microbial heavy-metal resistance. *Applied microbiology and biotechnology*, *51*, 730-750.

Nies, D.H. (2003). Efflux-mediated heavy metal resistance in prokaryotes. *FEMS microbiology reviews*, *27*(2-3), 313-339.

Oğuz, T.C. (2015). İçme Suyu Arıtımında Yaygın Olarak Karşılaşılan Su Kalite Problemleri ve Arıtımı İçin Çözüm Önerileri. *Orman ve Su İşleri Bakanlığı*, 92p. Ankara,

Pontius, F.W., Brown, K.G. & Chen, C.J. (1994). Health implications of arsenic in drinking water. *Journal-American Water Works Association*, *86*(9), 52-63.

Shankar, S., Shanker, U., & Shikha. (2014). Arsenic contamination of groundwater: a review of sources, prevalence,

health risks, and strategies for mitigation. *The scientific world journal*, *2014*(1), 304524.

Selinus, O., Alloway B., Centeno J.A., Finkelman R.B., Fuge R., Lindh U. & Smedley P., (2005). Essentials of Medical Geology. Impacts of the Natural Environment on Public Health. xiv + 812 pp. Amsterdam: Elsevier.). ISBN 0 12 636341 2. doi:10.1017/S0016756806002305

Smedley, P. L. & Kinniburgh, D. G. (2002). A review of the source, behaviour and distribution of arsenic in natural waters. *Applied geochemistry*, *17*(5), 517-568.

TS 266 (2005). ICS 13.060.20, Sular-İnsani Tüketim Amaçlı Sular. Türk Standartlar Enstitüsü, Ankara, Türkiye

US Department of Health and Human Services (2006). Agency for Toxic Substances and Disease Registry-ATSDR.

US Department of Health and Human Services. (2007). Agency for Toxic Substances and Disease Registry-ATSDR.

US EPA (2014). Office of Health, & Environmental Assessment. Exposure Assessment Group. (1989). *Exposure factors handbook* (Vol. 90, No. 106774). Office of Health and Environmental Assessment, US Environmental Protection Agency. http://iaspub.epa.gov/tdb/pages/general/home.do.

US EPA (2018). Drinking Water Standards and Health Advisories Tables.

Wang, S., & Mulligan, C.N. (2006). Occurrence of arsenic contamination in Canada: sources, behavior and distribution. *Science of the total Environment*, *366*(2-3), 701-721.

WHO (1993). *Guidelines for drinking water quality*, 2nd ed. Recommendations. World Health Organization.

WHO (2003). *Iron in Drinking-water Background document for development of WHO Guidelines for Drinking-water Quality*. Geneva: World Health Organization.

WHO (2011a). *Guidelines for Drinking Water Quality. 4th edn.* Geneva: World Health Organization.

WHO (2011b). *Arsenic in Drinking-water Background document for development of WHO Guidelines for Drinking-water Quality*. Geneva: World Health Organization.

WHO (2011c). *Manganese in Drinking-water Background document for development of WHO Guidelines for Drinking-water Quality.* Geneva: World Health Organization.

WHO (2011d). *Selenium in Drinking-water Background document for development of WHO Guidelines for Drinking-water Quality*. Geneva: World Health Organization.

WHO, U. GEMS (1989) Global freshwater quality. Published on behalf of the World Health Organization/Unites Nations Enviroment Programme, Oxford, Blackwell Reference.

CHAPTER III

Paleoenvironmental Conditions of Evaporites and Factors Determining These Conditions

Pelin GÜNGÖR YEŞİLOVA

1. Introduction

Evaporites are chemical sedimentary rocks that are the result of cooling and evaporation. All materials that are directly deposited from water as a result of evaporation are included in the definition of evaporite. Although they have a lower volume than carbonate rocks, evaporites, which were formed during different geological periods, can occasionally be hundreds of meters thick. These sediments, which are common in arid climate zones, are left behind, particularly after sea water evaporates. A portion of the evaporites end up in the water of arid basins on land. Some are deposited as byproducts of ocean water or pore water in sediments that form along the shore. Certain evaporites are created when evaporite minerals replace non-evaporite minerals in rocks that have already formed.

A high rate of evaporation, a dry and hot climate, a completely or semi-closed basin that allows salty waters to

concentrate, the intermittent or continuous inclusion of seawater mass in the basin, and mechanisms that will create the physical conditions for the accumulation of these evaporites are all necessary for the precipitation of geologically significant evaporite successions. The density and salinity rise as the water's volume decreases due to evaporation, and the minerals precipitate in a sequential order of decreasing solubility. For instance, calcium carbonate, calcium sulfate, sodium and potassium chlorides, and sodium, potassium, and magnesium salts precipitate, respectively, when seawater heated to 40^0C is periodically cooled. Calcite, which is equal to the density of water at a value of 1.0506, starts to precipitate when sea water drops to 53.3% of its initial volume. At that point, 19% of the gypsum (1.1304), halite (9.5%), and bittern salts (roughly 1.3%) are still present (Valyashko, 1962) (Figure 1).

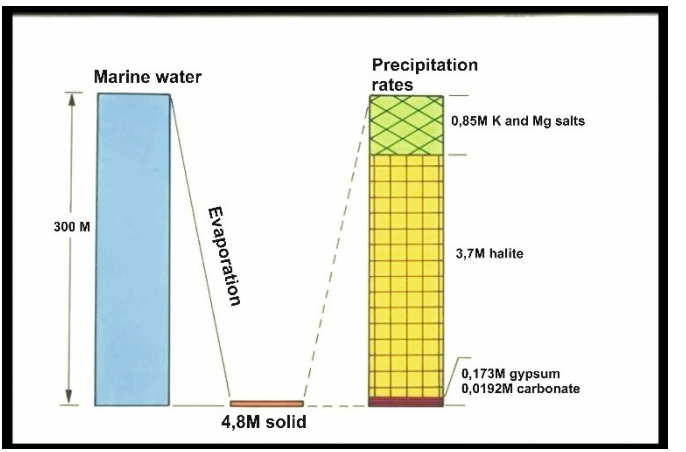

Figure 1. Components precipitated due to evaporation of sea water (modified Handford, 1991)

The most important feature of evaporite sedimentation is that it shows a zoning. This zoning is a sequence where the most difficult to dissolve sediments are distributed from the coast to the middle of the basin, while the most easily dissolved sediments are distributed in the middle of the basin (Figure 2). This type of zoning is called the ox-eye structure. The calcium carbonates and sulphates with the least solubility are deposited on the shelf, at the edge of the basin, although it is still largely covered by the sea. Later, the residual solution, enriched by sodium and potassium chlorides and other potassium salts, fills the central part of the basin (Figure 2). As an evaporite basin evaporates, it is drawn inward over time and the concentration increases in the middle. In the formation of basin-centered salt sediments; factors such as the basin being significantly subsided compared to the surrounding shelves and the absence of large volumes of terrigenic clastics must occur.

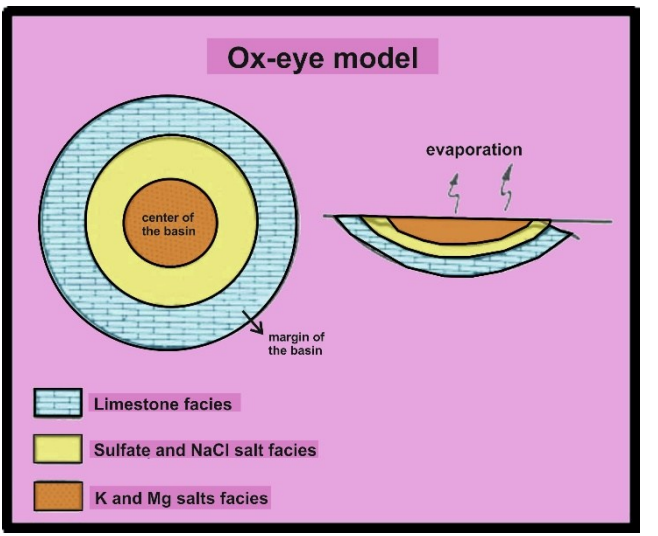

Figure 2. Evaporite facies deposited from the margin of the basin towards its center (ox-eye model) (modified Nichols, 2009).

2. Evaporite depositional environments

Evaporites can form in continental and marine environments. Some evaporitic lithofacies and sedimentary structures are very important in understanding these types of basins (Figure 3).

2.1. Evaporites deposited in continental environments

The primary basins where continental evaporites are deposited are swamps, lakes, playa lakes, temporary lakes, continental sabkhas, mud flats, salt pans, and mountain slopes where groundwater seeps (Figure 3). Continental basins are found in the valleys of mountain ranges and are grouped in the hydrological centers of closed basins (Figure 4, 5). They are not associated with any particular elevation. The underlying basement may appear as a muddy salt surface, depending on the degree of evaporation (Kendall, 1978). On the edge of playa lakes, behind the shores of coastal sabkhas, are lacustrine sabkhas, which are home to continental or marine sediments from past epochs. Sabkha formations are composed of sand, silt and clay (Figure 3). They are deposited by water that does not flow continuously from graben slopes or by winds blowing from the north. Sabkha surfaces slope inward from the edge of the depression (Figure 4, 5). The deposits in the middle of the depression are almost horizontal (Kendall, 1978).

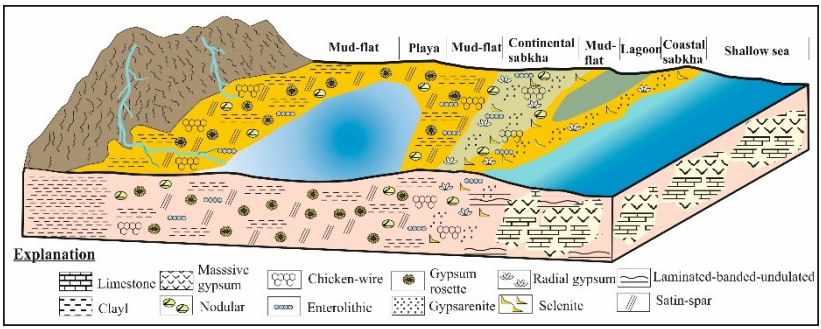

Figure 3. Marine and continental evaporitic environments and their sediments (modified Yavuz, 2021)

Some evaporites may be parallel or cross-bedded, laminated and ripple-marked. The observation of such structures indicates the shallow parts of the lakes. In addition, the observation of evaporite types such as discoidal gypsum, gypsum arenite, selenitic gypsum and chevron gypsum, nodular and bedded halite determine the shallow parts of these lakes (Schreiber & et al., 1976) (Figure 3).

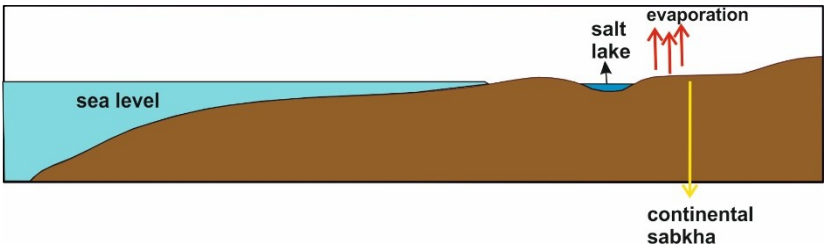

Figure 4. Continental sabkha model.

Figure 5. Yotvata continental sabkha (Amiel & Friedman, 1971)

Another continental depositional environment, playa, is a Spanish word meaning the shore or coast of a body of water. Marshes and lakes formed in the plains between mountains are evaporite formation areas and are called playa or playa lake (Figure 3, 6). Playas are formed by groundwater and are shallow depressions (Figure 6, 7). They are covered with a thin layer of water during the rainy season. There is no external discharge into the playa depression (Kendall, 1978). This has the lowest topography of the existing area. In such areas, material is only displaced by infiltration, evaporation and wind drift (Figure 7). The sediments forming the base of most playas are impermeable (Friedman & Sanders, 1978). Gypsum and caliche formations occur in the centers of playa basins.

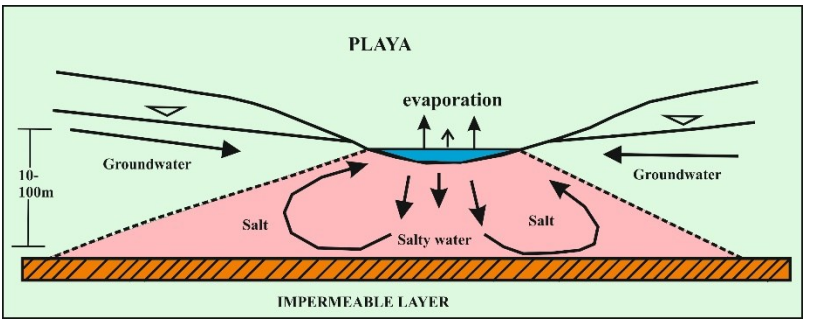

Figure 6. Groundwater recharge that provides salt precipitation in the playa system (modified Yechieli, 2000)

Salt pans are shallow open pans used to evaporate brine for salt production. Evaporites are formed by the sedimentation of seawater into a pool (Figure 8). Pans are usually found near a salt source. In many terrestrial deposits (salt pits and coalesced mud flats), the morphology of salt pans is similar to that in marine conditions, but their mineralogy is different (Figure 8). The shape and size of the evaporites deposited here determine the origin and amount of organic matter.

Figure 7. Ephemeral dried playa lake.

Figure 8. Santa Pola (Spanish) saline pans (Schreiber, 1978).

2.2. Evaporites deposited in marine environments

Various salt beds with high solubility, metal sulfide beds and some oil beds have formed in marine evaporite environments. Marine evaporites can deposit in supratidal salty mud flats or coastal sabkhas, lagoons, in deep seas and in drying basins (Figure 3, 9). Wide coastal plains bordering the lagoon are called coastal sabkhas. Thick evaporite beds dominated by carbonate sulfate beds are formed here. It is used for salt flats or salt marshes that are occasionally flooded by the sea but do not completely cover them (Figure 9).

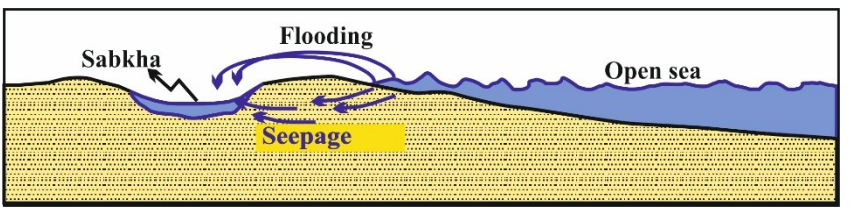

Figure 9. Coastal sabkha model (modified Kendall, 1979).

The deposition in marine (coastal) sabkhas generally occurs from the sea to the land. Evaporite formation in coastal sabkhas depends on marine effects, groundwater, location of the groundwater table; sediments formed in the environment, climate and topography (Figure 9). The sequence in marine sabkhas is from bottom to top; carbonates at the base, rarely clastics (subtidal), stromatolites and gypsum (intertidal-shallow sea) and upwards; nodular anhydrite, laminated dolomite and anhydrites containing chicken-wire and enterolithic sedimentary structures and marl at the top (supratidal-sabkha) (Figure 10). The complete drying of the deep sea environment causes sabkha and salt formation all over the basin. In such very wide basins, bedded halite and anhydrite or laminated anhydrite deposition may occur in the water (Tucker, 1981).

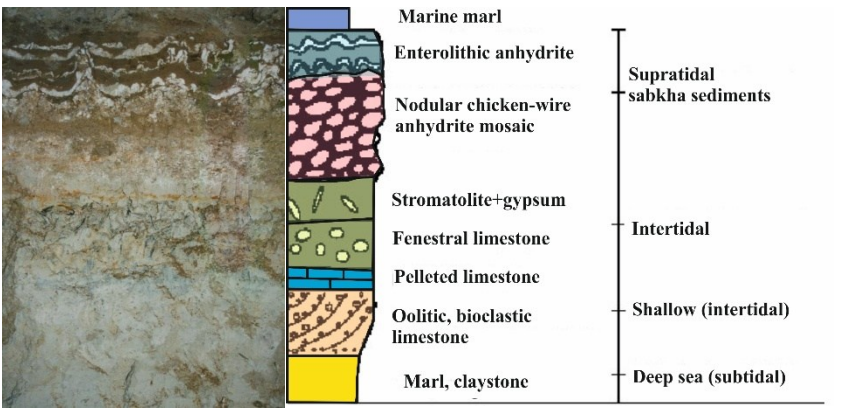

Figure 10. Supratidal salt flat model (modified Tucker, 1981).

The most important factor required for the development of evaporite successions in deep-sea environments is the presence of sedimentary barriers due to the development of structural, reef or sand banks controlled by faults that will divide the basin into small, isolated sub-basins (Tucker, 1981) (Figure 11). In such an

environment, the succession should consist of fine-grained sediments containing sapropel, indicating that the barrier has begun to form, and laminated anhydrite-gypsum deposits that have developed widely enough to be followed for kilometers, indicating that the barrier has completely shown its effect and that evaporation has begun. On the laminated anhydrite, there should be halite (which may contain anhydrite laminates in places), indicating that the basin is completely isolated and has begun to close. Just before the basin closes and its water dries up completely, K+ and Mg+ salts precipitate (Figure 11).

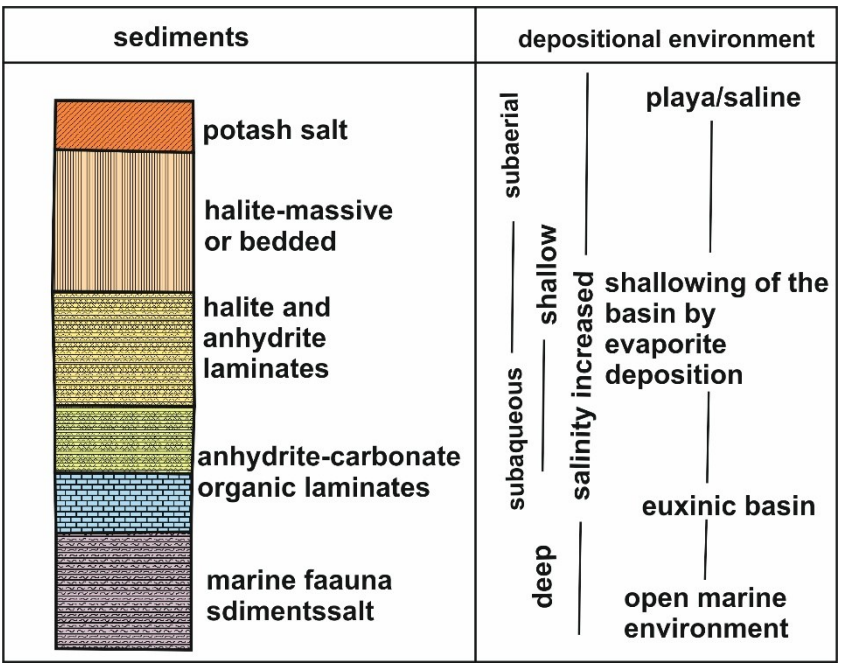

Figure 11. Generalized section of an evaporitic basin that started as an open-sea deepwater environment and subsequently closed. (modified Tucker, 1981).

In the drying deep basin model, evaporation must be greater than a point where the sum of recharge and sedimentation is at its highest level (Figure 12). These areas must be separated from the open sea by a shallow barrier. The silt (bar) in the sea limits the flow of sea water into the basin and the shallow sill depth provides the development of suitable conditions for evaporite deposition (Figure 12). The density changes caused by evaporation are effective on the salt water circulation in the basin and constitute important stages of basin development (Hsü, 1977).

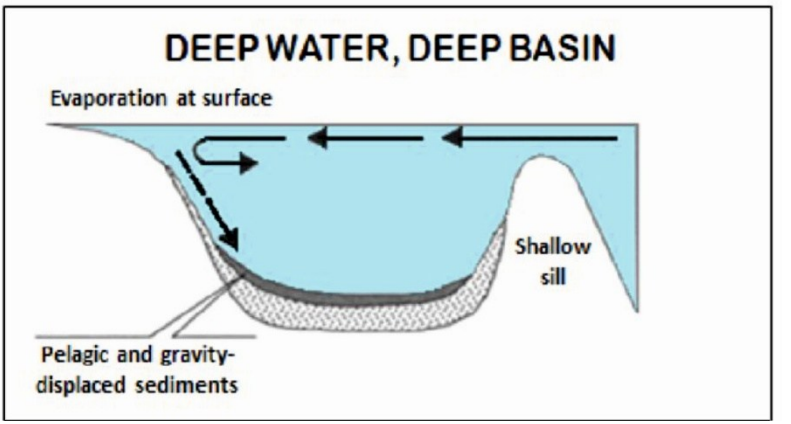

Figure 12. Drying deep basin model (taken from Mann &et al., 1999).

Along with these, it is another depositional area of evaporites in a lagoon or a wide shallow bay separated from an open sea by a physical barrier that can be overcome during abnormally high-water levels (Figure 13). Reef fragments that break off from the reef walls generally accumulate in front of and behind the reef and form barriers. These barriers prevent the free circulation of water on the shelf and provide the formation of evaporitic lagoon environments (Borchert & Muir, 1964). Almost all of the evaporitic formations

deposited in the lagoon environment originate from sea water. The lithology around the reef and back reef that forms the barrier symbolizes excessive salinity (Adams & Rhodes, 1960).

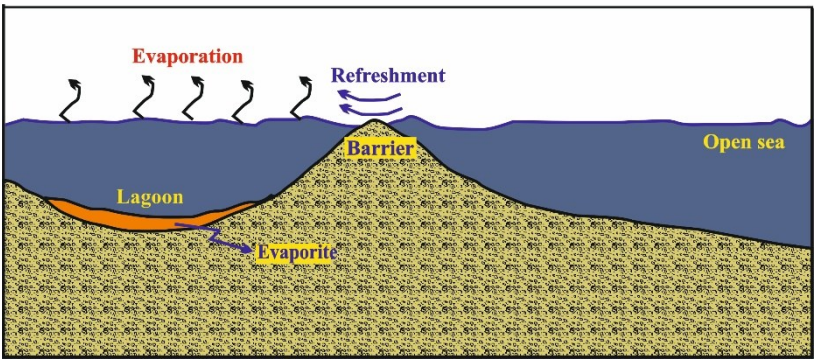

Figure 13. Barriered basin-lagoon model (modified Dean, 1978).

3. Factors determining paleodeposition conditions in evaporites

Some lithology (massive, laminated, nodular, radial, etc.), minerals (such as gypsum, anhydrite, celestine and halite), sedimentary structures (cross-bedding, ripples, enterolithic and chicken wire, etc.), grain size (such as gypsumrudite, gypsarenite and gypsite), organic matter content and type of twinning in evaporites provide evidence about paleodeposition conditions. Evaporites cannot remain stable in nature. Evaporite minerals, which are generally deposited directly from salt water in a primary form, are exposed to sedimentation and diagenetic processes (such as displacement, recrystallization, dissolution, cementation) under environmental conditions (such as temperature, pressure, tectonism, volcanism, diagenetics, underground, meteoric and hydrothermal fluids), replace each other and become secondary. These stages and the factors affecting the paleoenvironmental conditions can only be investigated through detailed sedimentary studies in the field,

microscopic petrographic (optical microscope) and mineralogical (Scanning electron microscope-Sem and X-ray diffraction-Xrd, etc.) studies. For example, radial type gypsums (Figure 14a) are formed by the effect of evaporitic ground water in lake shore marshes, supratidal areas and shallow environments (Cody, 1976; Hardie & et al., 1978). These gypsums appear as aggregations of fine gypsum crystals at wide angles in field and petrographic studies. These gypsums are formed when the ground water coming to the drying cracks formed in the claystone or carbonate mud flats that come to the surface during the drying stages of the environment becomes saturated for gypsum (Hardie & et al., 1978; Schreiber & et al., 1976; Magee, 1991).

Fibrous or satin-spar type gypsums (Figure 14b, c) develop in the fractures and cracks that occur during the transformation of anhydrite and gypsum into each other. It is evidence of effective dissolution and top pressure in the evaporitic environment. The observation of thick layered evaporites in the basin indicates that the external connection of the basin was cut off as a result of tectonic effects. Sand-sized evaporites (gypsarenite) (Figure 14d) generally accumulate in the margins of the basin. They are formed by the breaking, transportation and re-deposition of coarse-grained evaporites by wave action (Hardie & Eugster 1971, Aigner & Bachmann 1989). Primary gypsums lose their water due to the increase in temperature and salinity in the early diagenesis stage and begin to anhydrite with shallow burial. Thus, in sedimentary and petrographic studies, gray gypsum is observed as thin wires around white anhydrites and gives a texture like a chicken-wire (Murray, 1964; Shearman, 1978; Gibert & et al., 2007a) (Figure 14e). Nodular sulfates exposed to tectonism and pressure gain a ductile, fluid

feature. This type of texture takes on a enterolithic-like appearance (Shearman, 1963; Alsharhan & Nairn 2003; Warren, 2016) (Figure 14f).

Nodular anhydrites are characterized in petrographic thin sections by the coalescence and growth of primary anhydrite lats in an unconsolidated carbonate mud under the influence of increasing temperature and salinity during the syn-sedimentary stage (Schreiber & et al., 1976).

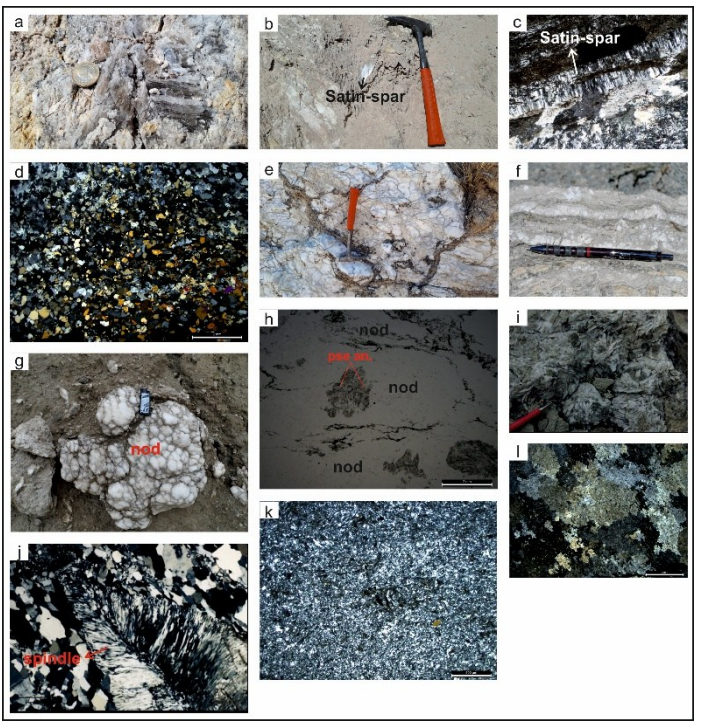

Figure 14. Various type of lithologic, sedimentary structures and optical microscope images of evaporites. (a, b) Twinned radial gypsum (darker parts contain organic matter), satin-spar gypsum within the mud (taken from Güngör-Yeşilova & Yavuz, 2021), (c) Crossed polars image of satin-spar gypsum perpendicular to

bedding, (d) Crossed polars image of clastic sand-sized gypsarenite, (e) Chicken-wire structure (taken from Güngör-Yeşilova, 2024) , (f) Enterolithic structure, (g) Nodular (nod) anhydrite in mud, (h) pseudomorphic anhydrite (pse an.) laths in the nodular (nod) anhydrite in the plane light, (i) glauberites that transform into secondary gypsum with alabastrine texture (taken from Gündoğan, 2000), (j) Crossed polars image of spindle-textured glauberite (taken from Gündoğan, 2000). (k) massive-microcrystalline texture, (l) Porphyroblastic texture (taken from Güngör-Yeşilova, 2020).

These may later be partially or completely transformed into secondary alabastrin and porphyroblastic textured gypsum as a result of early and/or late diagenetic processes. Nodular anhydrite is mostly formed in sabkha environment where continental conditions are dominant (Shearman, 1966) (Figure 14h). This type of texture is an indicator of a sabkha environment (Shearman, 1966). At the surface or near-surface regions, glauberite minerals transform into secondary gypsum (Figure 14i). These secondary gypsums may show spindle-shaped fibrous, network-shaped laminated, zigzag-shaped fibrous textures reflecting the transformation from glauberite to secondary gypsum in petrographic-mineralogical (SEM) studies (Figure 14j). Secondary gypsum textures are generally evident in petrographic studies as alabastrine, massive-microalabastrine (Figure 14k), microcrystalline massive, porphyroblastic (Figure 14l), nodular-chicken-wire, kataclastic, granoblastic, etc. texture types. This texture is formed by the dissolution and recrystallization of evaporite crystals by the salt water coming during the flood period (Holliday, 1970).

Some secondary gypsums are derived from the rehydration of anhydritized primary gypsums. The anhydritization process

manifests itself as synsedimentary or early diagenetic depending on salinity and temperature (Shearman, 1983). Pseudomorphic structures are present in some evaporites. In pseudomorphic structures, the shape of the mineral does not change but a mineralogical change occurs. This change also manifests itself depending on salinity and temperature (Hardie & et al., 1983). Their increase leads to the dissolution of the first evaporite mineral. Later, the migration of ions such as Na, Ca, Sr and cations such as CO_3^{-2} entering the mineral causes this displacement (Hovarka, 1992; Bell & Suarez, 1993). For example, anhydrite replaces calcite crystals (Figure 15a), halite cubes replace gypsum. Evaporite minerals have various sizes, shapes and colors, indicating the extent to which salinity, temperature, organic matter content, pH conditions and different water compositions (marine, fresh, brackish water) have mixed into the basin (Cody & Cody, 1989; Babel, 2004).

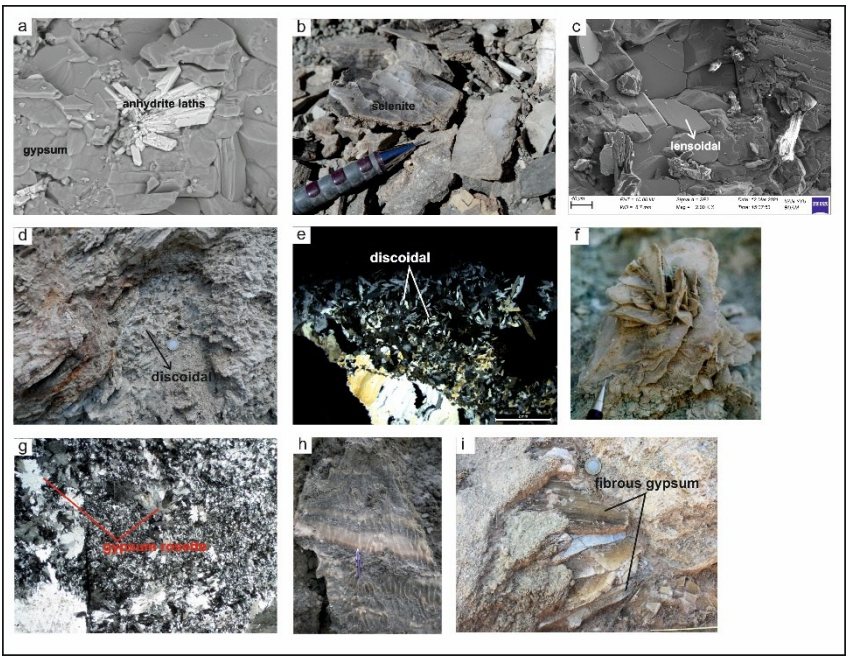

Figure 15. Various types of primary and secondary evaporite shapes. (a, b) Pseudumorphic anhydrite laths (after calcite) in the gypsums in the Sem and coarse-grained selenite containing organic matter (taken from Güngör-Yeşilova, 2020), (c) Sem image of lensoidal gypsum (taken from Güngör-Yeşilova, 2024), (d, e) image of land and crossed polars of discoidal gypsum, (f) Gypsum rosettes (taken from Gündoğan, 2000), (g) Crossed polars image of gypsum rosettes transforming into secondary alabastrine gypsum, (h) Banded-laminated halite and sylvite, (i) Fibrous gypsum in the carbonate.

For example, under high salinity conditions, the formation of coarse grain crystals (Figure 15b) of evaporite minerals is likely (Javor, 1983; Orti & et al., 1984; Geisler-Cussey, 1986, 1997). Tabular, lenticular, discoidal, rose-like and fibrious crystal shapes

(Figure 15c, d, e, f, g, h) can be attributed to increased organic matter content, slower crystallization rate and higher salinity, temperature and pH levels (Cody & Cody, 1989; Calvert & Pedersen, 1996; Aref & et al., 1997). The presence of banded or laminated an bedded halite (Figure 15i) supports the existence of a salt pan or lake environment subject to arid climate conditions, floods and dilution (Rosen, 1994; Lugli & et al., 2007).

The undulations, parallel laminations, load and flute structures, cross-bedding, fractures and folds in these evaporites reflect high energy shallow water conditions (such as lagoons) and presence of the tectonism (Reineck & Singh, 1975; Kendall, 1992; Orti & Rosell 2000, Tinterri & et al., 2016). (Figure 16a, b). In addition, in mineralogical studies, some organic materials (such as pellets, ooids, algae and bitumen, etc.) (Figure 16c) in evaporites may indicate subtropical and shallow water environments (Pryor, 1975; Tucker, 1981; Deik & et al., 2019). The existence of massive type evaporites (Figure 16d) indicates that there was an intensive underwater gypsum deposition and the basin deepened under the effect of tectonism (Hardie, 1984). In other words, this type of gypsum mostly shows the deep parts of the basin. Simple, chevron, swallow-tail twinnings in evaporites are accepted as the result of increasing pH, temperature and salinity of the environment (Aref & et al., 1997) (Figure 16e). The presence of some clay minerals (smectite, illite and caolinite, etc.) (Figure 16f) determined in evaporites in more mineralogical studies may provide information about climate and depositional conditions (Schnurrenberger & et al., 2003).

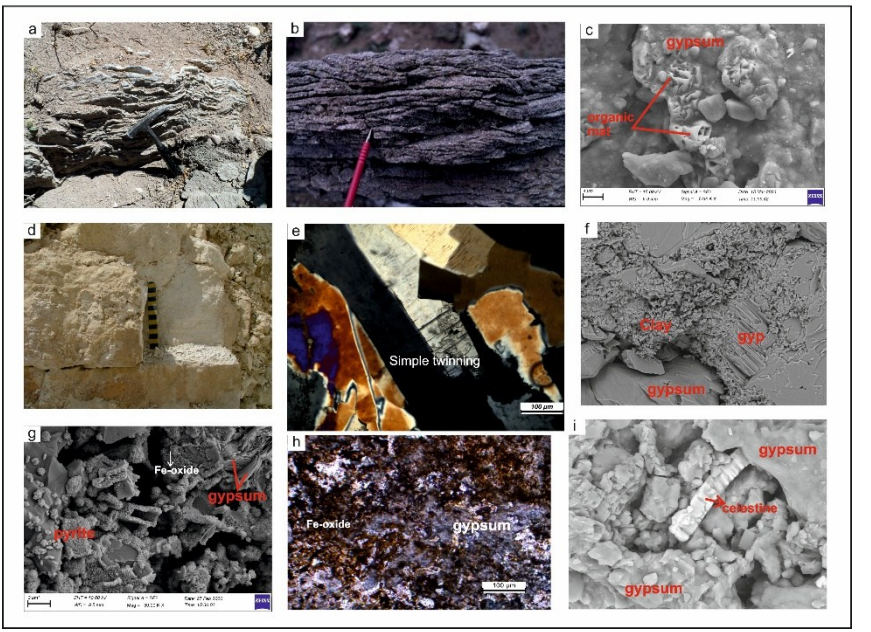

Figure 16. Microtexture and sedimentary structures in various types of sulphates. (a) undulations and microfolds in secondary laminated sulfates, (b) Cross-bedded of gypsarenite (taken from Gündoğan, 2000), (c) organic material (mat) in the gypsums in the Sem, (d) massive alabastrine textured gypsum, (e) Simple twinning of selenite crystals in the crossed polars, (f) Smectite type clay minerals within the gypsum in the Sem, (g) Microbial pyritization and iron oxidation in gypsum in the Sem (taken from Güngör-Yeşilova & Baran, 2023), (h) Reddish brownish iron oxidations in secondary gypsums with alabastrin texture in the crossed polars, (i) secondary celestine crystal replacing gypsum in the Sem.

For example, while smectite-type clay minerals indicate that the climate is subtropical or temperate, illite-type clays may support cold climate conditions (Kantorowicz, 1984). Again, the presence of other minerals such as feldspar, quartz, pyrite, calcite, dolomite and

Fe-oxide (hematite, pyrite and microbial pyrite, etc.) deposited together with evaporites provides insight into paleodeposition conditions (Figure 16g, h). For example, the presence of pyrite reflects anoxic conditions (Vallentyne, 1963), while the presence of minerals such as quartz and feldspar can be attributed to freshwater inflow, salt-freshwater mixing and solutions of different chemistry carried into the basin. Evaporite minerals may be primary or secondary due to diagenesis. They may undergo processes such as replacement and displacement by diagenetic processes. During late diagenesis, secondary calcite or celestine mixes with incoming carbonate or strontium-rich fluids and replaces sulfates (Figure 16i).

4. Conclusions

Evaporates accumulate and become deposited in semi-arid-arid regions, in extremely salty, bitter or very alkaline closed basins. In order for sedimentation to occur, the basin must be continuously fed by the relevant element through sedimentation, there must be very few streams that can bring fresh water to the basin and the evaporation rate in the region must be very high. Evaporites are formed in closed semiarid regions, in inland seas, in enclosed seas separated from the ocean by a shallow barriered, in lagoons, lakes, temporary lakes, marshes, sabkha, mud flats and on mountain slopes and foothills where groundwater emerges. In closed basins, the first element to start to precipitate is the less soluble salts that reach the saturation point first; and if the evaporation rate and material nutrition are suitable, compounds with high solubility precipitate. Thus, a series of compounds are precipitated. However, changes in environmental conditions such as the amount of water coming to the closed basin, its salinity, composition, temperature, evaporation rate,

concentration, nutrition possibilities, pH, anion-cation ratio may provide the successive precipitation of the same type of sediments, or a series of sediments consisting of different materials may form. Especially temperature and salinity are the most important factors controlling the composition of the precipitated salt. In fact, salts with different compositions may precipitate due to seasonal and even day-night temperature differences. In marine environments such as inland seas, closed seas and lagoons, where nutrition is slower than evaporation, hundreds of meters of rock salt, silvine, gypsum, anhydrite, calcite and nearly thirty Na, K, Ca and Mg compounds have been deposited. Primary and diagenetic sedimentary structures and lithologies in evaporites provide the most readable record of the depositional environment. Sedimentological, petrographic and mineralogical studies on evaporites reveal the extent to which evaporites are affected by climate, tectonism and diagenetic factors. With all these studies, the paleodeposition conditions of evaporites (organic matter effect, temperature, pH, fresh or bitter water inflow, pressure, etc.) are determined.

References

Adams, J. E. & Rhodes, M. L. (1960). Dolomitization by seepage refluxion. *American Association of Petroleum Geologists, Bulletin*, 44, 1912-1920.

Aigner, T., Bachmann, G. H. (1989). Dynamic stratigraphy of an evaporiteto- red bed sequence, Gipskeuper (Triassic), southwest German Basin. *Sed Geol*., 62, 5–25.

Al-Sharhan, A. & Nairn, A. (2003). *Sedimentary basins and petroleum geology of the middle east* (2nd ed.). Amsterdam: Elsevier.

Amiel, A. J. & Friedman, G. M. (1971). Continental sabkha in Arava Valley between. Dead Sea and Red Sea: Significance for origin of evaporites. *Bull. Amer assoc. Petrol. Geol*., 55, 581-592.

Aref, M., Attia, O. & Wali, A. (1997). Facies and depositional environment of the Holocene evaporites in the Ras Shukeir area, gulf of Suez, Egypt. *Sediment. Geol.*, 110, 123–145.

Babel, M. (2004). Models for evaporite, selenite and gypsum microbialite deposition in ancient saline basins. *Acta Geologica Polonica*, 54, 219–249.

Bebout, D. G. & Maiklem, W. R. (1973). Ancient anhydrite facies and environments, Middle Devonian Elk Point Basin, Alberta. *Bulletin of Canadian Petroleum Geology*, 21, 287-343.

Bell, C. M. & Suarez, M. (1993). The depositional environment and tectonic development of a Mesozoic intraarc basin, Atacama Region, Chile. *Geologica Magazine*, 130, 395–417.

Borchert, H. & Muir, O. R. (1964). *Salt deposits: The origin, Metamorphism and Deformation of Evaporites.* London: D. Van Nostr.

Calvert, S. E. & Pedersen, T. F. (1996). Sedimentary geochemistry of manganese: Implications fort he environment of formation of manganiferous black shales. *Econ. Geol.*, 91, 36–47.

Cody, R. D. (1976). Growth and early diagenetic changes in artificial gypsum crystals grown within bentonite muds and gels. *Geological Society of America Bulletin*, 87, 1163-1168.

Cody, R. D. & Cody, A. M. (1989). Gypsum nucleation and crystal morphology in analog saline terrestrial environments. *J. Sediment. Res.,* 582, 247–255.

Dean, W. E. (1978). Trace and minor elements in evaporites. In W. E. Dean & B. C. Schreiber (Eds.), *Marine evaporites*. (pp. 86-104). Tulsa: Society of Economic Paleontologists and Mineralogists.

Deik, H., Reuning, L., Petrick, B., Takayanagi, H. (2019). Hardened faecal pellets as a significant component in deep water, subtropical marine environments. *J Inter Assoc Sedim.,* https:// doi. org/ 10. 1002/ dep2. 64.

Friedman, G. M. & Sanders, J. E. (1978). *Principles of sedimentology*. New York: Freeman.

Geisler-Cussey, D. (1986). Approche se´dimentologique et ge´ochimique des me´canismes ge´ne´rateurs de formations e´vaporitiques actuelles et fossiles. Marais salants de Camargue et du Levant espagnol, Messinien me´diterrane´en et Trias lorrain. *Sciences de la Terre, Me´moires,* 48, 1–268.

Geisler-Cussey, D. (1997). Modern depositional facies developed in evaporative environments (marine, mixed, and nonmarine). G. Busson & B. C. Schreiber (Eds.) Sedimentary deposition in rift and foreland basins in France and Spain (Paleogene and Lower Neogene (pp. 3–42). New York: Columbia University Press.

Gibert, L., Ortı´, F. & Rosell, L. (2007a). Plio-Pleistocene lacustrine evaporites of the Baza Basin (Betic Chain, SE Spain). *Sed. Geol*., 200, 89–116.

Gündoğan, D. (2000). *Geology, mineralogy–petrography and economic potential of the Upper Miocene evaporites in the Beypazarı and Çankırı-Çorum basins*. İzmir: DEU, Fen Bilimleri Enstitüsü.

Güngör-Yeşilova, P. (2020). Bulanık (Muş) Paleojen evaporitlerinin petrografik- mineralojik incelemesi ve diyajenetik tarihçesi**.** *Maden Tetkik ve Arama Dergisi*, 162, 83-92.

Güngör-Yeşilova, P. & Yavuz, Ş. (2021). Sedimentological and mineralogical-petrographic characteristics of Miocene evaporitic deposits (SW Erzincan). *Manas*, 9*,* 169–183.

Güngör-Yeşilova, P. & Baran, O. (2023). Origin and paleoenvironmental conditions of the Köprüağzı evaporites (Eastern Anatolia, Turkey): sedimentological, mineralogical and geochemical Constraints. *Minerals*, 13, 282.

Güngör-Yeşilova, P. (2024). Genesis of sulfate lithofacies between Erzincan-Divriği Basin with sedimentologic and geochemical evidences: an example from the Paleogene basins of Eastern Turkey. *Carbonates and Evaporites*, 39:103.

Handford, C. R. (1991). Marginal marine halite-sabkhas and salinas. L. Melvin (Ed.), *Evaporite, petroleum and mineral resources, develop sediment* (pp. 50-66). Amsterdam: Elsevier.

Hardie, L.A. & Eugster, H. P. (1971). The depositional environment of marine evaporites a case for shallow, clastic accumulation. *Sedimentology*, 16, 187–220.

Hardie, L. A., Smoot, J. P. & Eugster, H. P. (1978). Saline lakes and their deposits: a sedimentological approach. A. Matter & M. E. Tucker (Eds.), *Modern and ancient lakes sediments* (pp.7-41), London, UK: Int. Assoc. Sedimentol. Spec. Publ.

Hardie, L. A. (1984). Evaporites: Marine or non-marine. *Amer Jour Scien*., 284, 193–240.

Holiday, D. W. (1970). The Petrology of secondary gypsum rocks: A review. *Journal of Sedimanter Petrology,* 40 (2): 734–744.

Hovarka, S. D. (1992). Halite pseudomorphs after gypsum in bedded anhydrite-clue to gypsum-anhydrite relationships. *Journal of Sedimentary Petrology*, 62, 1098-1111.

Hsü, K. J. (1972). Origin of saline giants, a critical review after the discovery of the Mediterranean evaporate. *Earth Science Review*, 8, 371-396.

Hsü, K. J., Montadert, L., Bernoulli, D., Cita, M. B., Erickson, A., Garrison, R.E., Kidd, R.B., Mèlieres, F., Müller, C. & Wright, R. (1977). History of the Mediterranean salinity crisis. *Nature*, 267, 399–403.

Javor, B. J. (1983). Planktonic standing crop and nutrients in a saltern ecosystem. *Limn. Ocean*, 28, 153–159.

Kantorowicz, J. D. (1984). Clastic diagenesis. *Geol Soc Lond Spec Publ*, 18, 189–226.

Kendall, A. C. (1978). Facies models 12: subaqueous evaporites. *Geoscience*, 5, 124–138.

Kendall, M. A. (1979). The stability of the deposit feeding community of a mud flat in the River Tees. *Estuar. Coastal Mar. Sci.,* 8, 15–22.

Kendall, A. C. (1992). Evaporites. A. C. Kendall (Ed.), *Facies models response to sea level change* (pp. 375–409). Canada: Geological Association of Canada.

Lugli, S., Manzi, V. & Roveri, M. (2007). New facies interpretation of the Messinian evaporites in the Mediterranean the Messinian salinity crisis from mega-deposits to microbiology a consensus report. *CIESM Workshop Monographs,* 7-10 November 2007, Almeria, (pp. 67-72).

Magee, J. W. (1991). Late Quaternary Lacustrine, groundwater, aeolian pedogenic gypsum in the Prungle lakes, Southeastern Australia. *Paleogeography, Paleoclimatology-Paleoecology,* 84, 3–42.

Mann, P., McLaughlin, P. P., Van den Bold, Jr. W. A., Lawrence, S. R. & Lamar, M. E. (1999). Tectonic and eustatic controls on Neogene evaporitic siliciclastic deposition in the Enriquillo basin, Dominican Republic, Caribbean basins. K. J. Hsii & P. Mann (Eds.), Sedimentary basins of the world (pp. 287-342). Amsterdam: Elsevier.

Murray, R. C. (1964). Origin and diagenesis of gypsum and anhidyrite. *Journal of Sedimantary Geology*, 34 (3), 512–523.

Nichols, G. (2009). Shallow marine carbonate and evaporite environments. Gary Nicholas (Ed.), Sedimentology and stratigraphy (pp. 225-245). Wiley, UK.

Ortí, F., Pueyo, J. J., Geisler-Cussey, D. & Dulau, N. (1984). Evaporitic sedimentation in the coastal salinas of Santa-Pola (Alicante, Spain). *Revista del Instituto de Investigaciones Geologicas*, 38/39, 169–220.

Orti, F. & Rosell, L. (2000). Evaporite systems and diagenetic patterns in the Calatayud Basin (Miocene, central Spain). *Sedimentology,* 47, 665–685.

Pryor, W. A. (1975). Biogenie sedimentation and alteration of argillaceous sediments in shallow marine environments. *Geol Soc Am Bull*., 86, 1244–1254.

Reineck, H. E. & Singh, I. B. (1975). *Depositional sedimentary environments*. Berlin: Springer.

Rosen, M. R. (1994). The importance of groundwater in playas, A review of playa classifications and the sedimentology and hydrology of playas. *Geological Society of America Special Papers*, 289, 1–18.

Schnurrenberger, D., Russell, J. & Kelts, K. (2003). Classification of lacustrine sediments based on sedimentary components. *J. Paleolim.*, 29, 141–154.

Schreiber, B. C., Freidman, G. M., Decima, A. & Schreiber, E. (1976). Depositional environments of upper Miocene (Messinian) evaporite deposits of the Sicilian Basin. *Sedimentology*, 23, 729-760.

Schreiber, B. C. (1978). Environments of subaqueous gypsum deposition. W. E. Dean & B. C. Schreiber (Eds.), *Marine evaporites. SEPM short course* (pp. 43-73).

Shearman, D. J. (1963). Recent anhydrite, gypsum, dolomite, and halite from the coastal flats of the Persian Gulf. *Proceedings Geological Society of London*, 1607, 63–65.

Shearman, D. J. (1966). Origin of marine evaporites by diagenesis. *Transactions of Institute of Mineralogy Metall.,* 75, 208-215.

Shearman, D. J. (1978). Evaporates of coastal sabkhas. W. E. Dean, B. C. Schreiber (Eds.) *Marine evaporates: SEPM Short Course* (pp. 6–42). Tulsa: Society of Economic Paleontologists and Mineralogists.

Shearman, D. J. (1983). Syndepositional and late diagenetic alteration of primarygypsum to anhydrite. *Sixth International Symposium on Salt*, 1, 41–50.

Tinterri, R. Muzzi-Magalhaes, P., Tagliaferri A. & Cunha, R. S. (2016). Convolute laminations and load structures in turbidites as indicators of flow reflections and decelerations against bounding slopes. Examples from the Marnoso-arenacea Formation (northern Italy) and Annot Sandstones (south eastern France). *Sediment. Geol.,* 344, 382–407.

Tucker, M. E. (1981). *Marine Evaporites.* New Jersey: Blackwell Sci. Publ.

Valyashko, M. G. (1962). *Geochemical regularities in the formation of potassium salt deposits.* Moscow: Izd. Mosk. Univ.

Vallentyne, J. R. (1963). Isolation of pyrite spherules from recent sediments. *Limnol. Oceanogr.*, 8, 16–30.

Warren, J. K. (2016). *Evaporites: A Geological Compendium.* (2nd ed.) Germany: Springer.

Yavuz, Ş. (2021). *Doruksaray-Dostal Köyleri (İliç-Erzincan) arasindaki evaporitik çökellerin litofasiyes özelliklerinin belirlenmesi*. Van: Yüzüncü Yil Üniversitesi Fen Bilimleri Enstitüsü.

Yechieli, Y. (2000). Fresh–saline groundwater interface in the Western Dead Sea area. *Ground Water,* 38, 615-623.

CHAPTER IV

İlk İnsanların Kullandığı Taş Aletlerin Jeolojik Özellikleri

Esin ÜNAL [1]
Çetin YEŞİLOVA [2]

Giriş

Evren var olduğundan beri zaman kavramı vardır. Her bilim dalı kendi alanında kapsadığı dönem ile ilgili zamansal sınıflamalar geliştirmiştir. Evrenin oluşumundan bu zamana yapılan en eski zaman sınıflaması yer bilimlerine aittir. Yer bilimlerinde kabul gören zaman cetvelinden önceki dönem Hadeen olarak adlandırılır. Bu dönem 4,5 milyar yıl olarak tarihlenen evrenin oluşumunu da kapsar. Hadeen döneminin ardından Prekambriyen döneminin başlamasıyla jeolojik zaman cetveli başlar ve günümüz son jeolojik

[1] Dr.Esin Ünal, Van Yüzüncü Yıl Üniversitesi, Mühendislik Fakültesi, Jeoloji Mühendisliği Bölümü, Van/Türkiye, Orcid: 0000-0002-8337-4651, esinunal@yyu.edu.tr
[2] Doç.Dr.Çetin Yeşilova, Van Yüzüncü Yıl Üniversitesi, Mühendislik Fakültesi, Jeoloji Mühendisliği Bölümü, Van/Türkiye, Orcid: 0000-0002-8884-0842, cetinyesilova@yyu.edu.tr

dönemi Kuvaterner'e kadar gelir yaklaşık 3.8 milyar yıllık bir süreyi sınıflandırır bu zaman cetveli. Antropoloji ve Arkeoloji gibi insan kökenli bilim dallarına geldiğimizde ise tarih öncesi çağlar olan "*Taş devri ve Maden devri*" ile ilgilenirken, Tarih bilimi ise Tarih çağları denilen "*ilk çağ, orta çağ, yeni çağ ve yakın çağ"* dönemleri ile ilgilenir.

Tarih öncesi veya Prehistorya (Latince, præ = önce + Yunanca, ιστορία = tarih), insanlığın yazının bulunmasından önceki dönemidir. Yazılı tarih öncesi olarak da bilinen prehistorya, yaklaşık 3,3 milyon sene önce ilk insanların taş aletleri ilk kez kullanması ile yazılı dilin icadı arasındaki zaman dilimini ifade eder (Anonim, 2024). Turkana (Kenya)'da bulunan en eski taş alet 3.3 milyon olarak tarihlendirilmiştir (Harmand & ark., 2015). Bu malzemenin eolit mi yoksa bir hominid, primat yada ilk insanlar tarafından şekillendirmeyle mi yapıldığı konusunda tartışmalar devam etmektedir. Jeolojik zaman cetvelinde bu dönem Üst Plisosen - Kuvaterner dönemine denk gelir ve Üst Pliyosen – Pleyistosen – Holosen devrelerini kapsar (Tablo 1). Afrika'da Üst Pliyosenin sonlarında ilk taş aletlere ait bulgular vardır. Anadolu'ya baktığımızda ise en eski taş alet Dursunlu (Konya)'da bulunan 900000 yıl olarak tarihlendirilen kuvarsit yongadır (Güleç & ark., 2003).

Jeolojik materyallerden yapılan aletler başlıca el baltaları, taş bıçaklar, kazıyıcılar, ok ve mızrak uçları olarak sayılabilir. Taş aletler, Paleolitik Çağ'da başlamıştır ve Kalkolitik Çağ'a kadar yaygın olarak kullanılmıştır.

Paleolitik Çağ, 2.5 milyon yıldan son buzul çağı sonu olan MÖ 12000 yıla kadar olan dönemi kapsar. Eski Taş Çağı, Kaba Taş Çağı ya da bilimsel adıyla Paleolitik, insan elinden çıkan ilk ürünler olan taş aletlerin yapıldığı çağdır. Bu taş aletler, en eski teknoloji (işçilik) ile temsil eder (Oldovan ve Aşölyen).

Tablo 1. Taş aletlerle ilişkili zamanların gösterimi (Kısmi jeolojik zaman cetveli, tarihöncesi ve tarih dönemleri).

<table>
<tr><td rowspan="15">Kuvaterner</td><td rowspan="13">Holosen
MÖ 12000 yıl - günümüz</td><td colspan="4"></td><td>Yakın Çağ</td></tr>
<tr><td colspan="4"></td><td>Yeni Çağ</td></tr>
<tr><td rowspan="7"></td><td rowspan="6">Maden Devri</td><td rowspan="2">Demir Çağı
MÖ 1190 –
MÖ 330</td><td>Le tene</td><td>Orta Çağ</td></tr>
<tr><td>Halstat</td><td rowspan="4">İlk Çağ</td></tr>
<tr><td rowspan="3">Tunç Çağı
MÖ 3300-
MÖ 1200</td><td>Geç Tunç Çağı</td></tr>
<tr><td>Orta Tunç Çağı</td></tr>
<tr><td>Erken Tunç</td></tr>
<tr><td rowspan="6">Taş Devri</td><td rowspan="3">Bakır Çağı
(Kalkolitik Çağ)
MÖ 5000-
MÖ 3000</td><td>Geç Kalkolitik</td><td rowspan="6"></td></tr>
<tr><td>Orta Kalkolitik</td></tr>
<tr><td>Erken Kalkolitik</td></tr>
<tr><td>Yeni Taş Çağı
MÖ 9000-MÖ 5500</td><td>Cilalı Taş Çağı
/Neolitik</td></tr>
<tr><td>Orta Taş Çağı
MÖ 12000-MÖ 9000</td><td>Epipaleolitik</td></tr>
<tr><td>Pleyistosen</td><td rowspan="3">Eski Taş Çağı/
Yontma Taş Çağı
2.5 My-MÖ 12000</td><td>Üst Paleolitik</td></tr>
<tr><td rowspan="2">Neojen</td><td>Üst Pliyosen
3.6 -2.5</td><td>Orta Paleolitik</td></tr>
<tr><td>Alt Paleolitik</td></tr>
</table>

Paleolitik Çağ insanlarının malzeme işleme teknolojileri, çakmak taşı ve diğer işlenebilir taşlardan, ayrıca hayvan kemikleri ve boynuzlardan oluşmaktaydı. Kemik ve boynuzların korunması jeolojik yapılara göre daha zordur. Bu sebeple kayadan yapılma aletlerin (taş aletler) günümüzde bulunabilmesi daha olasıdır. Taş alet kullanımına dair ilk arkeolojik kanıt yaklaşık 2,5 milyon yıl öncesine dayanmaktadır. (Semav & ark., 1997)

Epipaleolitik Çağ/Mezolitik Çağ (Orta taş devri), Son buzul çağından (MÖ 12000) tarımın başlamasına (MÖ 9000) kadar geçen süre Mezolitik çağ olarak tanımlanmıştır. Buzul çağından sonraki ılıman iklim koşullarına uyum sağlama evresidir. Mezolitik dönemde avcı toplayıcı olarak yaşayan topluluklar, taş baltalarının yanı sıra, özellikle çakmaktaşı ve çört gibi kayalardan yapılma mikrolit olarak mızrak ve ok uçları kullanılmıştır. Geç Paleolitikte kullanılan mikrolitler Mezolitik Çağ'da yaygınlaşmıştır.

Neolitik Çağ, (Cilalı taş devri) Tarımın başlangıcı MÖ 9000 ve Kalokolitik çağın başlangıcı MÖ 5000 arasındaki çağı temsil eder. Cilalı Taş, Yeni Taş çağı da denilmektedir. Bu dönemde çiftçilik, hayvan evcilleştirme ve yerleşik hayata geçiş başlamıştır. Taş aletler daha sert materyallerden yapılmıştır ve işçilik gelişmiştir. Çanak Çömleksiz Neolitik ve Çanak Çömlekli Neolitik dönem olarak ikiye ayrılır. Çanak Çömleksiz Neolitik dönemde Obsidyen taş aletleri ticarete konu olmuştur (Chataigner & ark., 1998).

Kalkolitik Çağ (Bakır çağı) Bu dönemde taş aletlerin yanı sıra bakır kullanılmıştır. Bakır taş çağı, Bakır Çağı da denilmektedir. MÖ 5000 – MÖ 3000 arasındaki dönemi temsil eder. Bakır çağını, sırasıyla Tunç çağı ve Demir çağı takip eder. Taş devri yerini maden çağına bırakır. Taş aletlerde işçilik ilerlemiştir kullanımı devam etmektedir ama azalmıştır.

Taş Aletler

Kayaçlar tek mineralden oluşabileceği gibi birden fazla mineralin bir araya gelmesi ile de oluşabilir. Tek mineralden oluşan kayaçlara mineral kayaç denilir. Minerallerin sahip olduğu özellikler meydana getirdiği kayacın özelliklerini de belirler. Talk gibi sertlik derecesi 3 (MOHS sertlik skalasına göre) olan bir mineralden oluşan kayaç yumuşak olur. Sabun taşı da denilen talk minderlinden oluşan bir kayaç yontulması ve işlenmesi çok kolaydır, taş alet olarak kullanılamaz ama süs eşyaları yapımında kullanılabilir. Minerallerin fiziksel özellikleri vardır. Renk, sertlik, kırılma yüzeyi, saydamlık, parlaklık, iletkenlik vb. Bu özelliklerden bir veya birkaçına sahip olan kayaçların taş alet yapımına uygun olduğu ilk insanlar

tarafından keşif edilmişti. Taş alet yapımında yontma, şekil verme için kullanacağınız malzeme ne çok sert ne de çok yumuşak olmamalıdır. Keşfedilen taş aletlere baktığımızda konkoidal kırılma özelliği gösteren ve sertliği yüksek (MOHS ≤ 7) kayaçlar ilk insanlar tarafından, yaygın olarak alet yapımında tercih edildiği görülmektedir. Taş aletin hangi malzemeden yapılacağının seçiminde fiziksel özelliklerinin yanında hammadde erişimi de etkili olmuştur. Bazalt, obsidyen gibi volkanik kayadan taş alet yapılması için bunu işleyen toplumların volkanik aktivitenin görüldüğü bölgelerde yaşamış olması gerekir.

Bu özelliklere sahip taş alet yapımına uygun olan jeolojik materyaller ve ne amaçla kullanıldıkları aşağıda belirtilmiştir.

Radyolarit (Radiolarite) Denizel zooplankton olarak bilinen radyolaryaların silisli kabuklarından oluşan, kompak (sıkı) silisli bir sedimanter kayaç (Çiftçi, 2003). Radyolaryalar öldükten sonra silis kavkıları derin deniz tabanın çöker ve birikerek radyolaritleri oluşturur. Kırılma yüzeyi ve sertliği nedeniyle taş alet yapımına uygundur. Anadolu'da Karain mağarası buluntularında saptanmıştır. Antalya ve civarında Karain, Öküzini, Suluin mağaralarında tespit edilen Neolitik aletlerin büyük çoğunluğu radyolaritten yapılma taş aletlerdir (kaynak). Alet yapımında az oranda çakmaktaşı ve obsidyen kullanılmıştır. Radyolaritlerin kaynağı ise Toros dağlarını oluşturan Bozkır birliği ve Antalya birliği üyesi Kayabaşı ve Alakır çayı, Çatal tepe gurubuna dahil radyolarit çökelleridir (Özgül, 1976). Derin deniz koşullarını yansıtan kırmızı renkli, çakmaklı pelajik kireçtaşı ve radyolaritleri kapsar. Bunlardan bazıları, toplam 20-30 m. kalınlık göstermelerine karşın Jürasik'ten Üst Kretase'ye kadar hemen bütün katları temsil eden mikrofauna kapsarlar ve bu özelliklerini yitirmeden yüzlerce kilometre yanal devamlılık gösterirler (Özgül, 1976).

Şekil:1 Radyolarit örneği (Lamotte, 2017)

Kalsedon (Chalcedony) Mikroskobik gözenekli, küçük kuvars kristallerinden oluşan, kriptokristalin silis çeşitlerinin grup ismi; bileşimleri SiO_2 'den $SiO_2.H_2O$'ya değişir. Akik, çört, opal, oniks, jasper ve çakmaktaşı çeşitlerini kapsar (Çiftçi, 2003). Kalsedon genellikle mumsu veya camsı bir parlaklığa sahiptir ve beyaz, gri, mavi ve kahverengi renklerinde bulunabilir.

İzmir, Aliağa bölgesinde yer alan Ege gübre antik yerleşim alanında bulunan taş aletler kalsedon ve çakmak taşından yapılmıştır. Ancak Ege bölgesi Palelolitik dönemi çok fazla çalışılmamıştır. Ege gübre kazısı dışında çakmaklı bölgesinde 2 farklı lokasyonda Paleolitik dönem bulgusuna rastlanmıştır ancak detaylı çalışma halen yapılmamıştır. (Erbil, 2018)

Çört (Chert) mikrokristalin kuvarstan oluşan oldukça kompakt ve sert olan çok sayıda kayaç için kullanılan bir isimdir. Çoğu çörtler. cam gibi konkoidal bir kırılma yüzeyine sahiptir. Çörtlerin sertliği, yontma kolaylığı ve keskin kenarlara sahip olmaları onları nedeniyle mücevher, mızrak ve ok yapımında kullanılmıştır. (Anonim, 2024) Hem çört (demir içeren) hem de çakmak taşının tarih boyunca ateş çıkarıcı özelliği kullanılmıştır. Çakmak taşı çörtün basit bir türüdür.

Şekil:2 Çört el baltası örneği Orta Paleolitik (https://stonetoolsmuseum.com/artefact/europe/mousterian-handaxe-3/3508/).

Çakmaktaşı (Flint) Siyah veya gri renkli, masif, sert, kirli kalsedon çeşidi. Konkoyidal kırılma yüzeyleri verir ve ateş taşı olarak bilinir (Çiftçi, 2003). Yaygın olarak Neolitik Çağ'da kullanılmıştır. Mikrolit olarak adlandırılan özellikle ok ve mızrak ucu gibi santimetre boyutunda aletlerin yapımında çoğunlukla çakmaktaşı kullanılmıştır. Mezolitik (Epipaleolitik) dönemde kullanımı yaygın aletlerin materyali çakmaktaşıdır.

Şekil:3 Çakmaktaşı El baltası örneği Orta Pileyistosen (https://stonetoolsmuseum.com/artefact/europe/acheulean-handaxe-14/6336/)

Kuvarsit (Quartzite) Esas olarak kuvars içeren ve çoğunlukla kuvars kumtaşlarının metamorfizması ile oluşan metamorfik bir kayaçtır (Çiftçi, 2003). Kuvars sertliği 7 olan mineraldir. Çoğunlukla taş balta yapımında kullanılmıştır. Taş baltası Alt- Orta paleolitik taş aletlerindendir (Tablo 1).

Şekil:4 Kuvarsit el baltası örneği (https://stonetoolsmuseum.com/artefact/africa/acheulean-handaxe-2/1135/).

Obsidiyen (Obsidian) Dasit ve riyolit bileşiminde volkanik cam. (Çiftçi, 2003). Dasit ve riyolit SiO_2 oranı yüksek lavlardan türemiş volkanik kayalardır. Onlarla aynı bileşime sahip lavların hızlı soğuması ile lav cam özelliği kazanır. Volkanlardan püsküren silis içeriği yüksek lavların hızlı soğuması sonucu camsı özellik meydana gelir. Bu camsı özelliği kayaca bıçak kadar keskin bir form kazandırır. Konkoyidal kırılma yüzeyleri oluşturur. Çoğunlukla siyah ve kahverengi, nadiren yeşil renk tonlarında bulunabilir. Anadolu kökenli obsidyenlerden yapılan taş aletler Neolitik dönemde hem Anadolu'da kullanılmış hem de ticareti yapılmıştır (Chataigner & ark., 1998).

Şekil:5 Obsidyen çekirdek örneği Kalkolitik (https://stonetoolsmuseum.com/artefact/west-asia/core-12/2392/)

Bazalt (Basalt) SiO_2 içeriği %52-45 arasında olan, volkanik kayaç. Obsidyen gibi volkanik aktivitenin görüldüğü alanlarda bulunur. Bazaltların yapısı volkanik aktivitenin püskürme tipine göre farklılıklar gösterir. Volkanın püskürttüğü lavın bileşimindeki uçucu gazların fazla olması bazaltın gözenekli olmasına sebep olur. Çünkü lav yüzeye çıktıktan sonra soğuma aşamasında bileşimindeki uçucu gazlar ayrılır, hava kabarcıkları gibi gözenekler oluşturur. Eğer magma odasından yüzeye ulaşan lav afirik yapıda ise camsı (afirik) dokuda bir bazalt meydana gelir. Bu tip afirik bazaltların alet yapımı açısından işlenmesi daha kolaydır. Bazalttan yapılma el baltaları oldukça yaygındır.

Şekil:6 Bazalt çekirdek örneği.
(https://stonetoolsmuseum.com/artefact/africa/oldowan-core/1151/)

KAYNAKÇA

Anonim (2024). *Chert*. (Aralık 2024 https://tr.wikipedia.org/wiki/Çört)

Anonim (2024). *Prehistorya*. (Aralık 2024) https://tr.wikipedia.org/wiki/Tarih_öncesi

Aydın, Y. (2018). Karain Mağarası Tayacian Alet Endüstrisi Tekno-Tipolojisi. *DTFC Dergisi*, *58*(2), 1327-1346.

Çiftçi E. (2003).*Yer Bilimleri Teknik Terimler Sözlüğü (İngilizce-Türkçe)*. (1.Baskı) Niğde. ISBN: 9789752880703.

Chataigner, C., J.L. Poıdevin, N.O. Arnaud. (1998). Turkish Occurrences of Obsidian and use by Prehistoric Peoples in the Near East from 14,000 to 6000 BP. *Journal of Volcanology and Geothermal Research 85*, 517–537.

D. Braun et al., (2019). Earliest known Oldowan artifacts at >2.58 Ma from Ledi-Geraru, Ethiopia, highlight early technological diversity. *Proc. Natl. Acad. Sci. U.S.A. 116*, 11712–11717.

Erbil E. (2018). Ege Gübre Neolitik Yerleşimi Ok Uçları Tekno-Tipolojisi. *Anadolu Arkeolojisinde Taş Aletler*. (229-243). İstanbul: Ege Yayınlar

Güleç, E., Howell, C., White, T., Karabıyıkoğlu, M. (2003). Anadolu'da İlk İnsan İzleri: Dursunlu, *Antropoloji Dergisi, 15*: 79-90.

Lamotte A., Chanson M.J., Wilemann G., Galtier F. (2017). Handaxes and leafpoints of eastern France: Spatial patterns and role of the raw materials. *Quaternary International, 428*, 79-90.

Museum of Stone Tools (2024). *Oldowan Core.* (10.12.2024 tarihinde https://stonetoolsmuseum.com/artefact/africa/oldowan-core/1151/ adresinden ulaşılmıştır).

Museum of Stone Tools (2024). *Obsidian core*. (10.12.2024 tarihinde https://stonetoolsmuseum.com/artefact/west-asia/core-12/2392/ adresinden ulaşılmıştır).

Museum of Stone Tools (2024). *Quartzite hand axe*. (10.12.2024 tarihinde https://stonetoolsmuseum.com/artefact/africa/acheulean-handaxe-2/1135/ adresinden ulaşılmıştır).

Museum of Stone Tools (2024). *Flint hand axe* (10.12.2024 tarihinde https://stonetoolsmuseum.com/artefact/europe/acheulean-handaxe-14/6336/ adresinden ulaşılmıştır).

Museum of Stone Tools (2024). *Chert hand axe*. (10.12.2024 tarihinde https://stonetoolsmuseum.com/artefact/europe/mousterian-handaxe-3/3508/ adresinden ulaşılmıştır).

S. Harmand et al., (2015). 3.3-million-year-old stone tools from Lomekwi 3, West Turkana, Kenya. *Nature 521*, 310–315.

Özgül Necdet. (1976) Toroslar'm bazı temel jeoloji özellikleri. *Türkiye Jeoloji Kurumu Bülteni, 19*, 65-78.

Semaw, S., Renne, P., Harris, JWK, Feibel, CS, Bernor, RL, Fesseha, N. ve Mowbray, K.(1997) . 2.5-million-year-oldstone tools from Gona, Ethiopia. *Nature 385*, 333- 336.

CHAPTER V

Yeşilova Ofiyoliti Ultramafitlerinin Mineralojisi ve Jeodinamik Evrim

Ayşe Didem KILIÇ[1]

1.Giriş

Likya napları, Türkiye'nin güneybatısında, Beydağları Otoktonu ile Menderes Masifi arasında, Erken Langiyen zamanında, Beydağları Otoktonu üzerine yerleşmiş allokton konumlu bir birimdir. Farklı ortam koşullarını karakterize eden, birbiri üzerinde ekaylanmalı litolojileri kapsayan bu napları, Domuzdağ napı, Gülbahar napı, Tavas napı, Bodrum napı ve Marmaris ofitolit napı ve Yeşilbarak napı olmak üzere altı ana tektonik birliği kapsar (Şenel, 1997). Beydağları otoktonu (Triyas-Pliyosen), Marmaris napı (Maastrihtiyen-Danien) ve Teke/Likya nappeleri (Langiriyen), ege graben sisteminin içinde bulunur. Bölgedeki naplar, genel olarak Burdur ve Acıgöl grabenleri arasında farklı jeolojik zamanlarda bir araya gelmiştir. Marmaris ofiyoliti, Bodrum napı üzerinde bulunmaktadır. Bu ofiyolit, hem Bodrum napı hemde Tavas napı tabanında tektonik dilimler şeklindedir. Şenel ve arkadaşları (1987),

[1] Doç. Dr., Fırat Üniversitesi, Mühendislik Fakültesi, Jeoloji Bölümü, Elazığ/Türkiye, Orcid: 0000-0002-6804-6764, adkilic@firat.edu.tr

Likya Napları'nı alt, orta ve üst naplar olarak ayırır. Alt Naplar'ın farklı ortam koşullarında çökelmiş, aynı yaşta kaya birimlerinden, Orta Naplar'ın peridotit ve Üst Senoniyen yaşlı ofiyolitli melanj ve olistrostomlardan, Üst Naplar'ın ofiyolit napı, ofiyolitli melanj ve olistrostomlardan oluştuğunu belirtir. Likya naplarını oluşturan yapısal birimlerin stratigrafik ve tektonik ortam özellikleri, bu allokton kütlelerin Anadolu-Torid platformunun kuzey kenarından ve kuzeyinden yani İzmir-Ankara-Erzincan zonundan kaynaklandığını yansıtır.

Tetis okyanusunun kalıntılarının bir arada olduğu birçok kıta ve okyanus mozayiğinden oluşan bir kenet kuşağı sunan Türkiye jeolojisi içerisindeki ofiyolitler, Jura – Üst Kretase (173 – 83 My) dönemi içerisinde oluşarak kıta üzerine yerleştikleri birçok çalışmada belirlenmiştir (Okay & ark., 2001, Harris ve diğ. 1994,Thuizat ve diğ.1981, Çelik & ark., 2008, Dilek & ark., 1999, Delaloye ve Wagner, 1984, Parlak & ark.,1995, Parlak ve Delaloye, 1996, Önen, 2003). Candan ve diğerleri (2011b), Batı Anadolu'da yapmış oldukları çalışma ile Neotetetis Okyanusu'nun kapanması ile alakalı hazırlamış oldukları jeolojik modelde Neotetis'in kuzey kolunun yitimi sonucunda kapanmasıyla (Anatolid-Torid bloğu içerisinde yer alan Menderes Masifi, Afyon Zonu ve Likya Napları'nın yığışım prizması oluşturduğunu ve bunların ekaylanma sonucunda farklı derinliklere gömülüp bu gömülme derinliklerine bağlı olarak metamorfizmaya uğradıklarını belirtmişlerdir. Bazı araştırmacılar, Likya Nappelerinin yerleşiminin, Menderes Masifi'nin kuzeyinde bulunan Neotetis'in kuzey kolunun kapanışıyla ilişkili olduğunu belirtmiştir.

Yeşilova Ofiyoliti, İğdir Metamorfiti ve Kızılcadağ Ofiyolitik Melanjı, Marmaris napı içinde yeralan tektonik birliklerdir (1). Marmaris ofiyolit napı, genelde masif peridotit, dunit, gabro kayaçlarından oluşur. Yeşilova ofiyoliti ise, ultramafik (harzburjit), mafik kayaçlar (dünit, gabro) ve diyabaz dayklardan oluşmaktadır. Yeşilova ofiyolitinin petrografi ve petrolojisi üzerine birçok çalışma bulunur (Karaman, 1987, Özpınar, 1987, Döyen, 1989, Şenel & ark., 1989, Ersoy, 1990, Kurnaz, 1992, Özpınar &

ark., 1996, Kılıç, 2017). Yeşilova Ofiyoliti tektonitler, kümülatlar, bazik volkanikler ve tüm ofiyolit istifini kesen mafik damar kayaçları kapsar. Özpınar (1987), Yeşilova ofiyolitinin, harzburjit, lerzolit ve dünitten oluştuğunu, bu kayaçların gabro, norit, diyabaz, dolerit ve kuvarslı diyorit kayaçları tarafından kesildiğini ifade eder. Yeşilova ofiyoliti, Lütesiyen-Oligosen arası bir zaman aralığında bölgeye tektonik olarak yerleşmiştir. Araştırmacı, Yeşilova ofiyolitinin tabanında bulunan metamorfik kayaçların ise, ofiyolitin yerleşimi sırasında tabandan ve yan kayaçlardan koparılan amfibolit, kuvarsit, kalkşist ve yeşilşist görünümlü metamorfik kayaçlar olduğunu ve bu kayaçların ofiyolitik melanj içerisinde, blok ve mercek şeklinde konumlandığını belirtir. Melanj içerisinde, kısmen metamorfizma geçirmiş Üst Kretase yaşlı pelajik kireçtaşları ve Üst Kretase-Paleosen yaşlı fliş yeralır. Bilgin ve diğerleri (1990), Kızılcadağ Ofiyolitli Melanjı/olistrostomunun Üst Senoniyen ve Yeşilova-Tefenni Ofiyoliti' nin Mesozoyik yaşlı olduğunu ifade eder. Yıldız ve Ayhan (1992), Kurnaz (1992), Kızılcadağ Melanjı'nın Paleozoyik-Mesozoyik yaşlı olduğunu ve serpantinit ve amfibolit blokları, bazalt, pelajik kireçtaşları, radyolarit şist, volkanoklastik hamuru içinde bulunur (Kılıç, 1996, Kılıç ve Karaca, 2021).

Yeşilova ofiyolitinin tabanında yeralan metamorfitlerinde yapılan çalışmalardan biri, Elitok ve Drüppel (2008) tarafından, Beyşehir-Hoyran Ofiyoliti tabanındaki tektonik dilim şeklindeki metamorfik dilimin, alkali ve toleyitik karakterde olduğunu ve 630-770 °C sıcaklık, 6 ± 1.5 kbar basınç koşullarında yaklaşık 18-20 km derinlikte oluştuğunu belirlemişlerdir. Bu sıcaklık ve basınç koşulları, Batı Anadolu ofiyolitlerinin İzmir-Ankara Süturu'ndan Akdeniz'e kadar geniş bir yüzeylemeye sahiptir. Bu ofiyolitlerin tabanındaki metamorfik dilimler, YB/DS metamorfizması sonucu oluşmuştur (Kılıç ve Güler, 2023). Çelik ve Chiaradia (2008), peridotitleri kesen ve metamorfizmaya uğramış dolerit ve amfibolit dayklarında yaptıkları çalışmada, kayaçların yitim zonunda farklı zamanlarda oluştuklarını ifade etmişlerdir. Kılıç (2012), Yeşilova Ofiyoliti tabanındaki amfibolitlerin petrografik ve petrolojik

özelliklerinden 700°C sıcaklık ve 10-11 kb basınç koşullarını işaret ederken, Parlak (2016) ve Parlak ve diğerleri (2019), Likya Ofiyolitleri'nin tabanında okyanus içi yitim sonucu dinamotermal metamorfizmanın geliştiğini ve metamorfik dilimin granat amfibolit, amfibolit, mikaşist, kalkşist ve mermerden oluşur. Metamorfizma, dilimin üst bölümünde amfibolit fasiyesi, alt bölümünde yeşilşist fasiyesi olduğunu ve ters metamorfik zonlanmanın geliştiğini belirtir. Ofiyolitik melanj ve peridotitler arasındaki tektonik metamorfik dilimin ölçülebilen kalınlığının 350 m kadar olduğunu ve metamorfik dilimdeki U-Pb ve Ar-Ar yaş analizlerinin benzer yaş göstermelerinin, okyanus içi yitimin başlangıcının metamorfik dilimin oluşum yaşını gösterebileceğini belirtirler. Kılıç (2020), amfibolit, mikaşist, kalkşist ve mermerlerden oluşan metamorfik dilimdeki granatlı amfibolitlerde $\delta_{18}O$ izotop değerinin % 4.2 bulunmuş olması, köken kayacın magmatik olduğunun göstergesidir.

Yeşilova ofiyoliti, Marmaris Napı içerisinde yer alan kökeni tartışmalı ofiyolitlerden biridir. 1813 yılında Fransız bilim insanı Brongniart tarafından jeolojiye kanzandırılan ofiyolit terimi, başlangıçta melanj içindeki serpentinitler için kullanılırken, 1821'de aynı araştırmacı, ofiyoliti, Alp-Appeninler'deki magmatik kayaçlar (ultramafikler, gabro, diyabaz ve volkanik kayaçlar) için kullanmıştır. Bugün bildiğimiz anlamda ofiyolit terimi ise Steinmann'a aittir (Ersoy,1990). Araştırmacı, Ligurya yaşlı Apennin serpentinitlerini ve onlarla birlikte bulunan ultrabazik kayaları, volkanik kayalarda magmatik farklılaşmanın ürünleri olarak yorumlamıştır. Magma farklılaşması ve yoğunluk farklarından kaynaklanan farklılaşma, ofiyolit birimine ait seviyelerin gelişmesinin nedenidir.

Bu çalışma kapsamında, Burdur ili, Yeşilova ilçesine bağlı Ulupınar ve İğdir köyleri çevresindeki ultramafik kayaçların petrografik ve petrolojik özellikleri ile mineral kimyasından bölge evriminin belirlenmesi amaçlanmıştır.

2. Yöntem

Saha çalışmalarında toplanan, yeşilova ofiyoliti ve metamorfitlere ait 60 kayaç örneğinin ince kesitleri, Fırat Üniversitesi laboratuvarlarında hazırlanmış ve mikroskop görüntüleri alınmıştır. Yeşilova ofiyolitinin farklı noktalardan alınan kaya örnekleri, ana oksit, iz element ve Nadir Toprak Elementi (REE) analizleri için, Tungsten-Karbür bileşimli halka değirmeninde 150-200 mikron büyüklüğünde öğütülmüştür. Her öğütme işleminden sonra, halka değirmeni alkol-su karışımı ile temizlenmiştir. Toz haline getirilen örnekler, ACME Analitik Laboratuvarı'nda (Kanada) İndüktif Çift Plazma-Kütle Spektrometrisi (ICP-MS) cihazı kullanılarak kimyasal analizlere tabi tutuldu. 0.5 g toz halindeki örnekler ICP-MS cihazı ile analiz edildi. Seçilen minerallerin elektron mikroprobu analizleri (EMPA), YEBİM'de (Ankara-Türkiye) yapılmıştır. Plajiyoklaz ve piroksenlerin kimyasal analizleri için, dalga boyu dağıtıcı (WDS) JXA8230 model JEOL marka cihaz kullanılmıştır. Hazırlanan ince kesitlerden EMPA analizi için iki örnek hazırlandı (plajiyoklaz ve piroksen içeren). Karbon kaplama ve cilalama işlemlerinin ardından ölçümler yapıldı ve ölçümlerdeki matris etkileri JEOL tarafından sağlanan ZAF yazılımı kullanılarak düzeltildi.

3. Bulgular

3.1. Jeoloji

Burdur ili Yeşilova ilçesi' ne bağlı uluova ve iğdir köyleri arasındaki ofiyolit ve metamorfitleri konu alan bu çalışma, literatürde Tefenni-Yeşilova Ofiyoliti, Marmaris Ofiyoliti ve Marmaris-Yeşilova Ofiyoliti gibi adlamalarla kullanılan yeşilova ofiyolitinin (Karaman, 1987, Özpınar, 1996), İğdir, Akçaköy, Örencik ve Armutköy köyleri arasını da büyük içine alan bölümünü kapsar. Çalışma alanının kuzeyinde Kızılcadağ Ofiyolitik Melanj ile güneyde iğdir metamorfitleri ile konumu tektoniktir (Şekil 1).

Yeşilova Ofiyoliti, harzburjit, lerzolit, dünit, gabro, plajiyogranit, diyabaz ve dolerit daykından oluşur (Özpınar & ark.,

1996) (Şekil 1).Dunitler ile harzburgitler arasındaki sınır geçişli olup, kromite yakın yerlerde bulunan dunitler, deformasyona uğramıştır (Şekil 3). Faylı alanlarda, ilerlemiş serpentinizasyon ve iyi gelişmiş bir elek yapısı, dunitlerde krizotil ve lizardit oluşumuna sebe olduğu görülür. Yeşilova ofiyolitinin tektonit birimlerini tamamen, kümülat seviyesini ise kısmen kesen bu damar kayaçlar, koyu siyah renkte olmaları ve topoğrafyada çıkıntı oluşturmaları sayesinde kolayca farkedilir. Tektonizma tüm ofiyolit birimlerini etkilemiştir (Şekil 4).

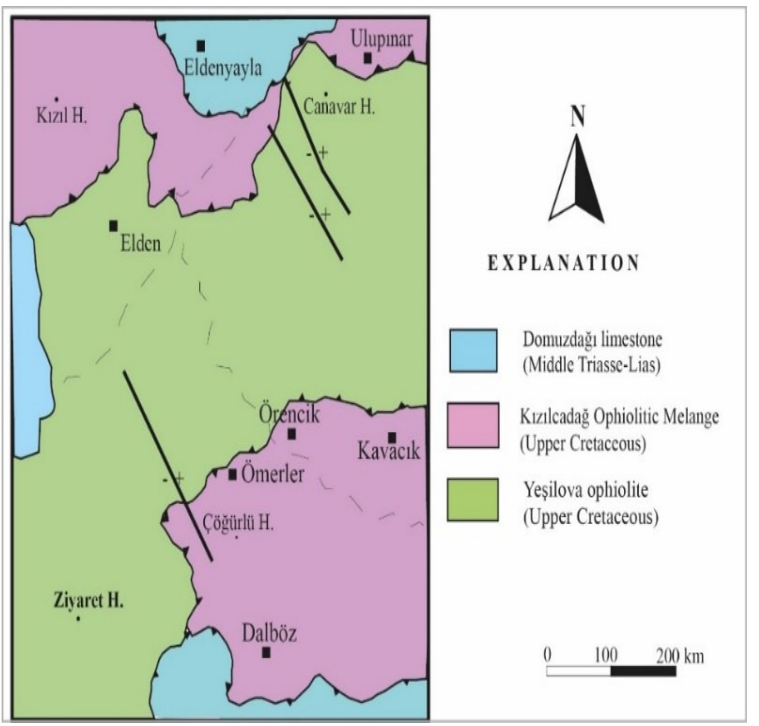

Şekil 1. *Çalışma alanının jeolojik haritası (Karaman, 1994'den değiştirilerek alınmıştır)*

Şekil 2. *Yeşilova ofiyoliti ultramafitlerinin arazi görünümü*

Yeşilova ofiyoliti birikimlerine yapılan K-Ar yaş analizleri, bu birimin yaşını yaklaşık 114 milyon yıl olarak vermiştir (Aksoy, 2008, Karaman, 1994). Bu birim, Geç Senoniyen döneminde kıtasal kabuğun üzerine itirilmiş olup, Neotetis'in kuzey kolunu temsil eden İzmir-Ankara-Erzincan Bölgesi'nden kaynaklandığını göstermektedir.

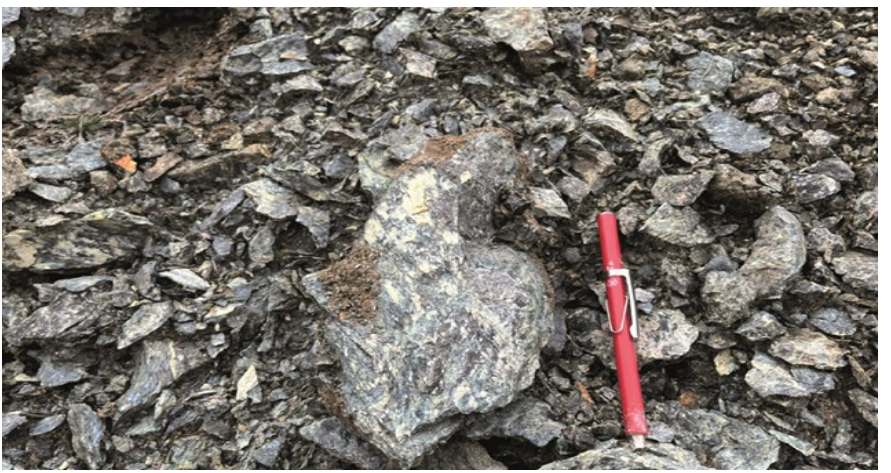

Şekil 3*. Serpantinitler ve serpantinize harzburjitlerin görünümü*

Kızılcadağ Melanjı ve Olistostrom, Girdev Melanjı, İç Toros Ofiyolitik Kompleksi, Gökçebağ Kompleksi, Isparta Ofiyolitik Karışımı gibi adlarla kullanılan Kızılcadağ Ofiyolitik Melanjı (Erkman, 1982,Thuizat, 1981,Koçyiğit, 1981,Şenel, 1997), okyanus kabuğuna ait temel volkanitler, neritik kireçtaşı, pelajik kireçtaşı, radyolarit, şist blokları ve serpentinit, serpantinleşmiş harzburgit ve dunit kayalarından oluşur. Kaotik bir içyapıya ve alacalı bir renge sahip bu birim, doğudan batıya doğru eğimli katmanlı yapı gösterir (Şekil 2). Tektonizma yoğun alterasyona özellikle lisvenitleşmeye sebep olmuştur (Şekil 5). Melanj ayrıca tektonizmden etkilenmiş ve birimler içinde kataklaz izleri oluşmuştur.

Şekil 4. *Yeşilova ofiyolitnde görülen lisvenitleşme*

3.2. Petrografi ve Petroloji

Yeşilova ofiyoliti, harzburgit, dunit, lherzolit, gabro ve bu birimleri kesen diyabaz daykından oluşur. Harzburgitler, taze örneklerde yeşil bir görünüm sergilerken, ileri derecede serpentinizasyona uğramış örneklerde sabunumsu kayganlık ve yeşilimsi siyah renk

gösterir. Tektonizma nedeniyle, bu kayaçların kırmızımsı oksidasyon yüzeyi ve serpantinleşme sebebiyle yeşilimsi-siyah renk ve yüzeyindeki kayganlık tipiktir. Harzburjitlerin mineral bileşimi olvin ve ortopiroksendir. Elek doku gelişmiştir.

Dünitler, karasız bir mineral olan olivin ve kromitten oluşur. Nodüler ve saçınımlı doku izlenir. Serpentinizasyon ve ani soğuma, yuvarlak bir şekil ve katman katman ayrılma geliştirmiştir. Genelde harzburjit ve serpantinitlerde izlenen soğan kabuğu ayrışmasını dünitlerin gösteriyor olması tektonizma etkisinin yüksek olmasından kaynaklanır (Oberhanslı & ark., 1997). Serpentinizasyon sırasında olivin, manto koşullarında kristalize olan bir anhidrat mineralidir. Olivin, atmosferik koşullarda kolayca değişime uğraması da soğan kabuğu ayrışmasının gelişmesinde katkı sağlamış olabilir. Genellikle, alterasyon dünit ve harzburjitlerin kenarları ve ince çatlakları boyunca başlar ve hızlı bir şekilde tüm kayaç yapısı değişir (Kılıç, 2012).

Şekil 6. *Serpantinize gabrolardan bir görünüm*

Tektonizmanın bir diğer sonucu, serpantinlerle birlikte görülen hematit mineralinin varlığıdır. Serpantin ve hematit mineraleri, olivin ve manyetit mineralinin hacim genişlemesi-sıkışma mekanizması ve ani soğumayla gelişen mekanizmanın sonucudur (Irvine, 1971, Zheng & ark.,2008b). Holokristalin ve hipidiomorf granüler dokuya sahip lerzolit ve harzburjitlerdeki olivin ve piroksenler, yüksek optik engebe ve canlı girişim rengi ile kolayca tanınır. Hidrotermal alterasyon, olivinlerde iddingsitleşmeye ve ilerleyen süreçte serpentinleşmeye sebep olur (Şekil 6). Simektit, klorit ve hematit türündeki ikincil mineraller, alterasyon sırasında hidrojen iyonlarının olivin yapısından uzaklaşmasıyla, ortamda rastgele oksijen iyonlarına bağlanan, Mg^{+2}, Fe^{+2} ve Si^{+2} katyonlarının bağlanma şekilleriyle yakından ilgilidir (Çelik,1999). Fe^{+2}'nin Fe^{+3}'e oksitlenmesi, ortamda opasitleşmeye neden olur ve kırık hatları boyunca opak mineraller gelişir (Şekil 7).

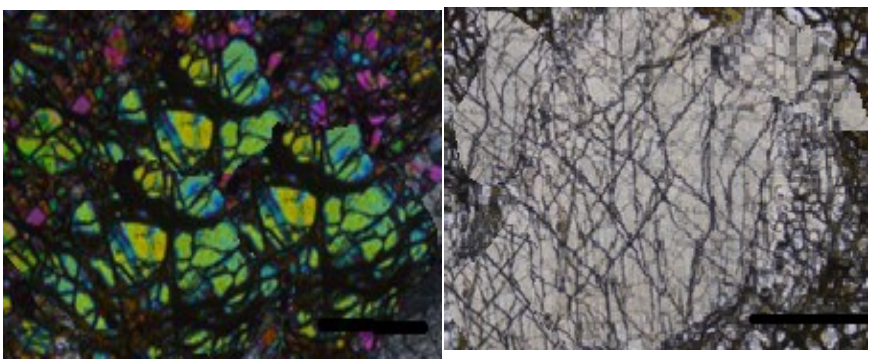

Şekil 7. *Harzburjitlerin mikroskop görüntüsü. Olivin (Ol) ve ortopiroksen (Opx)*

Serpentinize lerzolitleride, olivin, hidrotermal koşullar altında ve CO_2'li çözeltilerin etkisiyle kataklaz bir alterasyon gösterir ki; bu alterasyon merkeze doğru ışınsal kırılma boyunca gelişmiştir (Şekil 7). Yeşilova ofiyolitinin kümülat gabro seviyesi, tabakalı gabro, izotrop gabro, plajiyogranit ile bu kayaçları kesen klinopiroksenit ve diyabaz bileşimli dayklardan oluşur. Koyu siyah renk ve yüksek

sertlikte izotrop gabrolar, koyu ve açık renkli ve orta tane büyüklüğünde homojen bir dağılımına sahiptir. Birim tektonizma sebebiyle, kırıklı çatlaklı bir görünüm almıştır.

Çalışma alanındaki bir diğer birim, Yeşilova Ofiyoliti ile Kızılcadağ Melanj arasında yeralan, İğdir metamorfiti'dir. Ters metamorfizma özelliğine sahip bu birim, Yeşilova ofiyoliti ile sınırında metamorfizma derecesi üst amfibolit-granülit fasiyesi geçişi karakterindedir. Ancak, Kızılcadağ melanjı ile olan alt sınırı yeşilşist fasiyesi düşük sıcaklık metamorfizmasını gösterir. Dolayısıyla, düşük dereceli metamorfizmadan yüksek dereceli metamorfizmaya doğru değişim, yeşil biyotit + garnet (Sps) + muskovit + plajiyoklaz + kuvars ± zirkon ± opak mineral ve aktinolit + granat (Spesartin) + yeşil biyotit + muskovit + kuvars + plajiyoklaz + epidot + opak mineral parajenezinin gelişmesine sebep olur. Gabroların ayrıntılı petrografik incelemeleri, magma karışımının dokusal özellikleri ve mineral içeriğini etkilediğini göstermektedir. Poiklitik hornblend, plajiyoklaz, kuvars-hornblend/klinopiroksen gözlü dokusu, süngerimsi plajiyoklaz oluşumları ve apatit oluşumları homojen bir magma karışımını (mixing) işaret etmektedir. Bölgesel ölçekte düşünüldüğünde Orta Anadolu Kristalen Kompleksi içerisinde Neo-Tetisin kalıntı ürünleri olarak köksüz bloklar halinde değilde kristalen karmaşığa sokulum yapan eş yaşlı mafik-felsik magmalardan mafik magmanın kristalizasyon ürünleri olabileceği düşünülmektedir.

3.3. Jeokimya

Yeşilova ofiyoliti' ne ait kayaç örneklerinin jeokimyasal analiz sonuçları Tablo 1'de verilmiştir. Seçilmiş 12 gabro örneğine ait ana oksit, iz element ve nadir toprak elementi (NTE) analizlerinde, SiO_2 %38.85-50.13, Al_2O_3 %0.39-15.69, Fe_2O_3 %7.43-11.19, MgO % 5.10-43.64, CaO % 0.44-7.22 ve ateş kaybı değeri %1.14-6.59 dur.

Table 1: *Gabroların anaoksit, iz element ve nadir toprak element analizi*

	Dk-1	**Dk-2**	**Dk-3**	**Dk-4**	**Dk-5**	**Dk-6**	**Dk-7**
SiO_2	40.72	38.85	50.11	50.13	44.11	40.72	40.85
Al_2O_3	0.74	0.39	15.72	15.69	0.80	0.74	0.81
TiO_2	0.02	0.02	1.08	1.01	0.04	0.01	0.02
Fe_2O_3	8.33	7.68	8.30	11.19	8.10	7.43	9.11
MgO	42.12	43.64	6.18	5.10	42.12	42.12	42.15
MnO	0.11	0.09	6.19	6.14	0.15	0.12	0.19
CaO	0.84	0.44	5.55	7.22	1.04	0.67	0.72
Na_2O	0.01	0.02	3.11	3.02	0.01	0.02	0.01
P_2O_5	0.01	0.01	0.04	0.06	0.01	0.02	0.02
Ateş kaybı	4.36	6.59	1.72	1.14	3.04	6.02	6.11
Toplam	**97.26**	**97.13**	**98.00**	**100.7**	**99.42**	**97.87**	**99.89**
Rb	0.1	0.3	1.2	0.1	1.4	1.6	1.3
Y	0.4	2.8	18.1	19.2	0.7	0.3	22.0
Sc	12.4	1.3	3.1	25.7	12.1	8.5	111.4
Nb	0.1	1.4	0.6	0.1	0.7	1.1	0.8
Ba	27	2	43	1	46	62	12
La	0.50	2.40	0.70	2.60	3.70	2.80	3.10
Ce	0.20	7.40	6.80	0.50	0.55	7.30	0.20
Nd	6.20	6.70	0.30	5.90	5.40	6.90	0.30
Sm	1.76	1.89	0.88	2.31	1.99	0.05	0.10
Eu	0.02	0.70	0.90	0.02	0.68	0.50	0.04
Gd	2.71	0.05	3.12	0.05	2.77	3.35	3.21
Tb	0.01	0.60	0.51	0.52	0.02	0.01	0.60
Dy	0.08	0.07	3.44	4.08	0.09	3.75	0.06
Ho	0.02	0.85	0.73	0.02	0.66	0.58	0.26
Er	0.03	2.21	2.60	0.07	0.03	2.33	2.25
Tm	0.01	0.20	0.33	0.01	0.30	0.17	0.14
Yb	0.80	0.67	0.74	0.88	0.82	0.76	0.79
Lu	0.01	0.02	0.01	0.01	0.01	0.01	0.01
Ta	0.1	0.3	0.1	0.4	0.1	0.5	0.1
Hf	0.1	0.1	0.3	0.1	0.2	0.1	0.1
Pb	0.1	0.4	0.1	0.3	0.3	0.1	0.6
U	0.2	0.1	0.1	0.2	0.1	0.1	0.1

Toplam alkali-silika diyagramında, gabroların subalkalin alanda gabro bölümünde yer aldığı görülür. Ti/Y - Nb/Y diyagramına göre (Şekil 9), örneklerin bir örnek hariç toleyitik alanda yer alması, gabroların toleyitik magma ürünü olduklarının işaretidir.

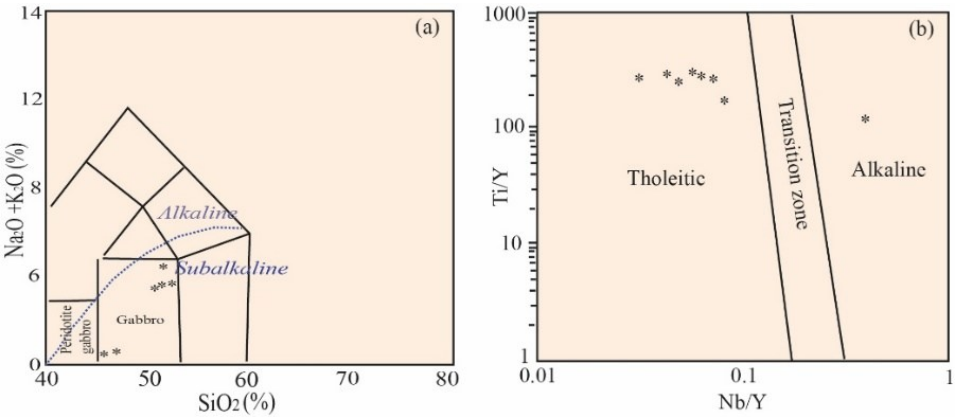

Şekil 8. Gabroların Alkali-silis diyagramı (Pearce, 1982) ile Ti/Y-Nb/Y diyagramları (Middlemost, 1986)

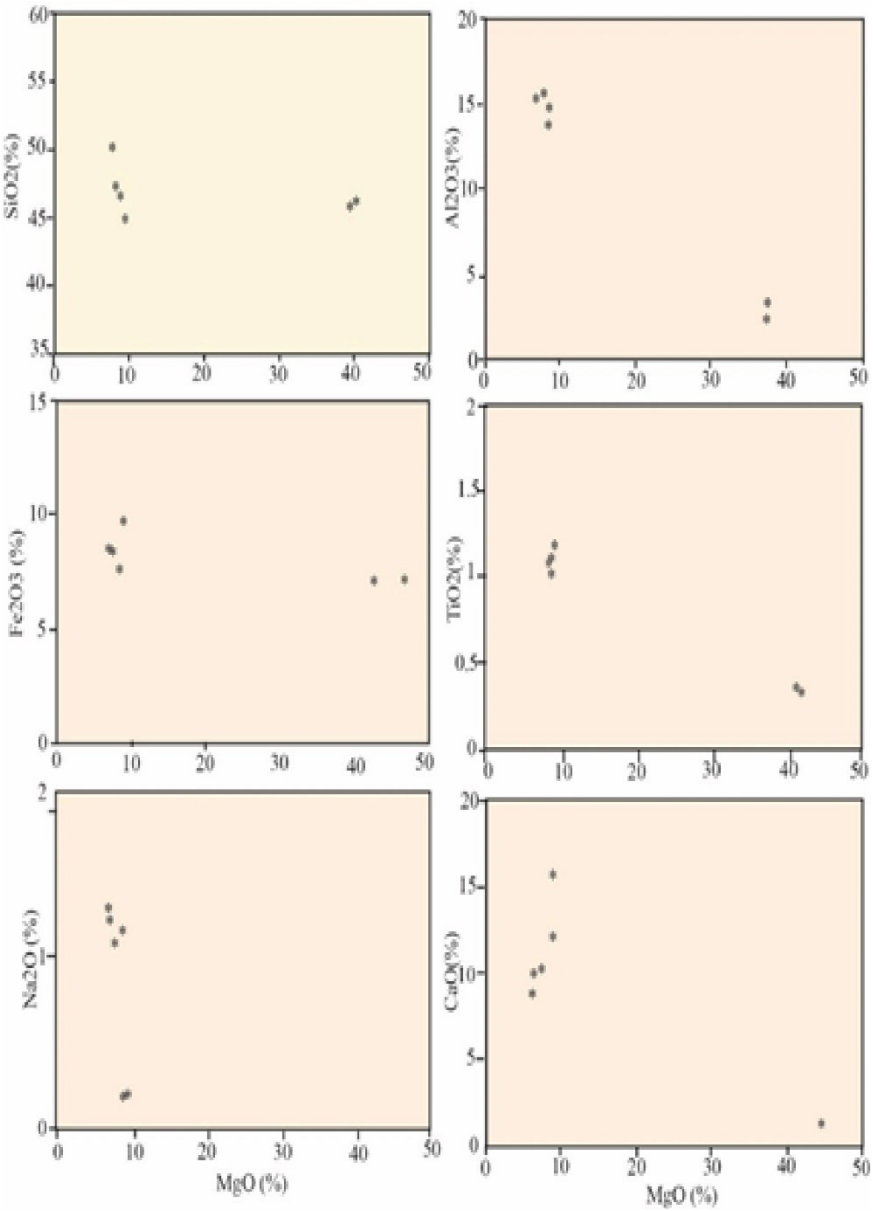

Şekil 9. *Gabroların diğer anaoksit-MgO dğişim diyagramları*

Seçilen gabroların, Şekil 9'da MgO'in diğer ana oksitlerle değişimini Harker diyagramları ile değerlendirilmiştir. Bu diyagramlarda, MgO ile SiO_2, Al_2O_3 arasında negatif korelasyon, Fe_2O_3, CaO, K_2O ve TiO_2 arasında pozitif korelasyon gözlenir (Şekil 9). Pozitif korelasyon gabro bileşiminden kaynaklanmaktadır. Bu korelasyon, mafik bir magmanın kristalleşme evrelerinde oluşan tek bir topluluğu işaret eder.

İz elementi diyagramlarının MgO'le karşılaştırıldığı diğer ikili diyagramlarda, gabroların V, Hf, Zn ve Rb elementlerinde pozitif artış izlenir. Bu diyagramlarda MgO bileşimi hemen hemen yakındır. Ancak, iz element oranları artış göstermektedir (Şekil 10 ve Şekil 11). Bu sonuçlar, mafik kayalardaki plajiyoklaz mineralinin fraksiyonlanmasını ve klinopiroksen ile Fe-Ti oksitlerinin kristalizasyonunu işaret eder. Ayrıca, V ve Hf'nin artışı, magmanın derin ve oldukça sıcak bir kaynaktan beslendiğini ve belirli mineral fraksiyonlamaları sürecine girdiğini gösterir ki; özellikle Hf, zirkon gibi minerallerde yoğunlaşma eğilimindedir. Gabrolarda, Zn ve Rb'nin artışı, hidrotermal etkilerin varlığını ve hidrotermal alterasyon süreçleri sırasında kayalarda zenginleşmeyi gösterir. Rb'nin artışı, magmanın alkali özelliğindn kaynaklanır ki, örneklerden birinin alkali alana düşmüş olması bunu doğrulamaktadır. Bu elementlerin artışı, magmanın belirli bir tektonik ortamda (okyanus ortası sırtları veya adalar yaylası) oluştuğunu ve toleyitik ve alkali bazaltlar arasında geçiş gösteren ortamların karakteristiğidir.

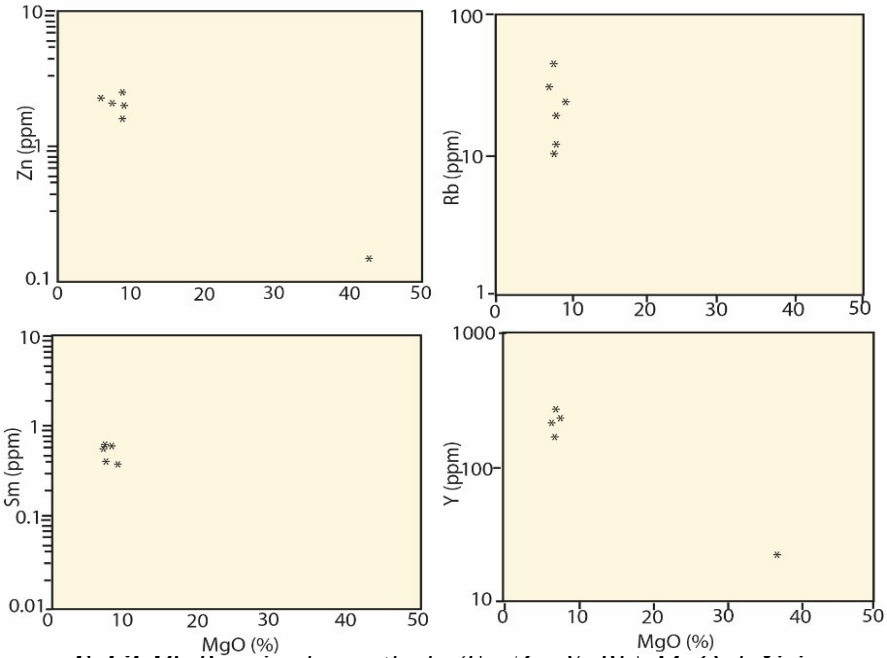

Şekil 10. *Bazı iz elementlerle (Sm,Zn, Y, Rb)-MgO değişim diyagramı*

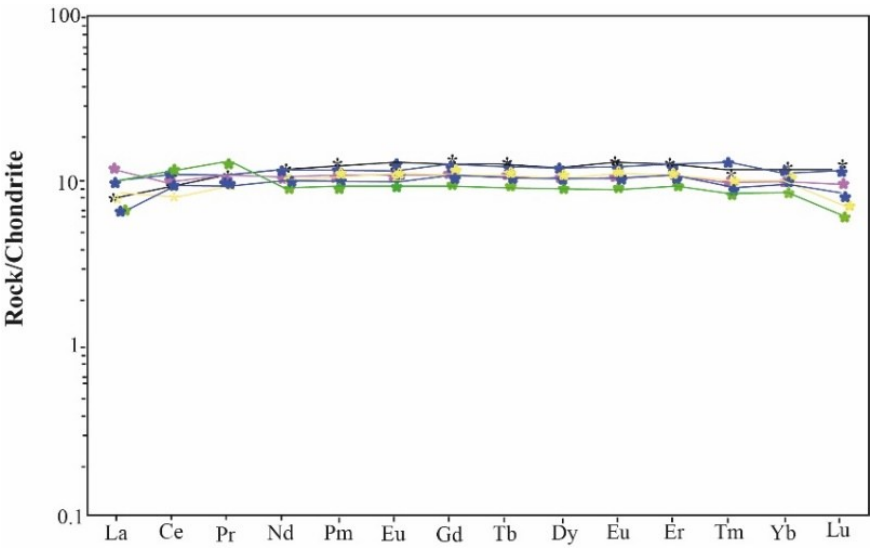

Şekil 11. *Gabroların Kondrite göre örümcek diyagramı*

3.4. Garbroların Mineral Kimyası

Yeşilova ofiyoliti gabro kayaları; mikrogabro, hornblend gabro ve tabakalı gabro olarak sınıflandırılabilir. Mikrogranüler ve granüler doku gösteren gabroların mineral bileşimi plajiyoklaz, klinopiroksen/amfibol ve olivin olarak belirlenmiştir (Şekil). Plajiyoklaz taneleri öhedral ve subhedral şekillerde bulunmaktadır. Plajiyoklaz kristallerinin kenarlarında ve ikiz izlerinde kalsit, albit ve zoisit gözlemlenmektedir. Piroksenler subhedral ve anhedral taneler şeklindedir ve plajiyoklaz ile sınırı ortaktır. Plajiyoklaz ve piroksen kırık izlerinde kloritler gelişmiştir. Amfibol ve kloritler küçük taneler (1-3 mm) halinde bulunur. Kloritler, genellikle piroksenlerin hidrotermal alterasyonu sonucunda gelişmiştir.

Petrografik incelemelerde, mikrogabrolar ve orta taneli tabakalı gabrolarda sosüritleşme izlenir. Sosiritleşme, plajiyoklazın hidrotermal alterasyonu sonucu gelişir. Orta taneli gabrolarda olivin, yalnızca klinopiroksen ve plajiyoklaz arasındaki kontakta bulunmaktadır. Hornblende gabrolar, %25 plajiyoklaz, %60 amfibol ve %15 klinopiroksen bileşimindedir. Ayrıca, apatit ve titanit ikincil mineral olarak bulunur. Gabrolarda amfibol oranının yüksek olması, magma kaynağındaki su içeriğine ve sıcaklık koşulları gibi faktörlere bağlıdır. Bu, magma asidik hale geldiğinde ortaya çıkabilir. Ayrıca, bu tür bir mineralojik dağılım, oluşum koşullarının hidrotermal etkinlikten etkilendiğini de gösterebilir. Mikrogabro genellikle daha küçük tanelere sahip olup, daha homojen bir mineral dağılımına sahiptir. Orta ince taneli gabrolarda ise, mineral taneleri daha büyük ve farklı kristalizasyon süreçlerinin etkisiyle daha belirgin olabilir. Bu farklılıklar, oluşum ortamındaki sıcaklık, basınç ve kimyasal bileşim gibi faktörlerden kaynaklanır (Koçak & ark., 2005). İri taneli amfiboller, kahverengi pleokroizm gösterir. Amfibol içeren gabroların dokusu granüler ve poikilitiktir. Tabakalı gabrolar subofitik bir dokuya sahiptir. Amfibollerin mineral birleşimleri, %15 klinopiroksen, %50 plajiyoklaz ve %35 amfibol'dür. Amfibol, subhedral ve anhedral fenokristler şeklindedir. Gabrolarda hidrotermal mineraller olarak epidot, klorit ve serisit gelişmiştir. Ayrıca, hornblende gabrolardaki çatlak ve kırıklarda ikincil kalsit ve

epidot oluşmuştur. Amfibol, biotit ve Fe-Ti oksitleri içeren birleşimlerin varlığı, bu gabroların su içeriği yüksek ve okside olmuş ilkel bir magmanın ürünü olduğunu göstermektedir.

Table 2: *Gabrolara ait klinopioksen ve plajiyoklasın EMPA sonuçları*

	Plajiyoklaz				**Klinopiroksen**		
Analizler	**Yf-1**	**Yf-2**	**Yf-3**	**Yf-4**	**Yc-1**	**Yc-2**	**Yc-3**
SiO_2	57.91	56.11	58.74	58.45	41.93	42.14	41.84
Al_2O_3	28.44	27.75	29.03	27.15	13.50	15.24	13.46
TiO_2	0.08	0.09	0.10	0.05	1.88	1.92	1.75
Fe_2O_3	0.35	0.39	0.54	0.62	11.22	11.33	15.94
Cr_2O_3	0.01	0.00	0.02	0.00	0.00	0.02	0.00
MnO	0.07	0.00	0.06	0.04	0.20	0.25	0.16
MgO	0.08	0.12	0.09	0.07	10.71	13.18	13.74
Na_2O	5.24	6.18	5.09	6.21	1.64	1.66	1.71
CaO	7.98	10.33	0.02	0.43	11.50	11.55	12.01
K_2O	0.44	0.47	0.09	0.44	0.81	0.86	0.72
F	0.15	0.08	0.13	0.20	0.07	0.11	0.03
Cl	0.05	0.03	0.02	0.09	0.10	0.06	0.10
Toplam	100.8	101.55	94.11	93.75	93.56	98.32	101.46

Kimyasal formülü $XY(Si,Al)_2O_6$ olan piroksenlerde, X (Ca, Na, Fe, Mg) ve Y (Cr, Al, Fe, Mg) katyonlarından oluşabilir. Tablo 2'de kimyasal analiz verileri sunulan gabrolara ait klinopiroksenler, Q($Ca^{+}Mg^{+}Fe^{2+}$) ve J(2Na) diyagramında kalsiyum bakımından zenginleştiği görülür (Şekil 13). Analiz edilen örneklerin bileşimi, $En_{42}Fs_8Wo_{42}$ ile $En_{48}Fs_{13}Wo_{47}$ arasındadır. Analizi yapılan piroksenlerin, diopsit ve ojit bileşimli olduğu belirlenmiştir (Şekil 12).

Tablo 2'de ana oksit bileşimleri verilmiştir. Bu analizler, yüksek TiO_2 (0.79-1.67%), Al_2O_3 içeriği 2.96–4.31%, Na_2O içeriği 0.23–0.40% ve Cr_2O_3 içeriği 0.04–0.76% olduğunu ve Mg# değerlerinin ise genellikle %77-86 arasında değiştiği görülür. Toplam Ca + Na ile Ti ikili diyagramında (Şekil 12c), alkali ve sub-alkali bazalt sınırında yer aldığı görülmektedir. Bu nedenle, gabroik kayalardaki klinopiroksenler, magmadan doğrudan kristalize olan birincil

minerallerdir.

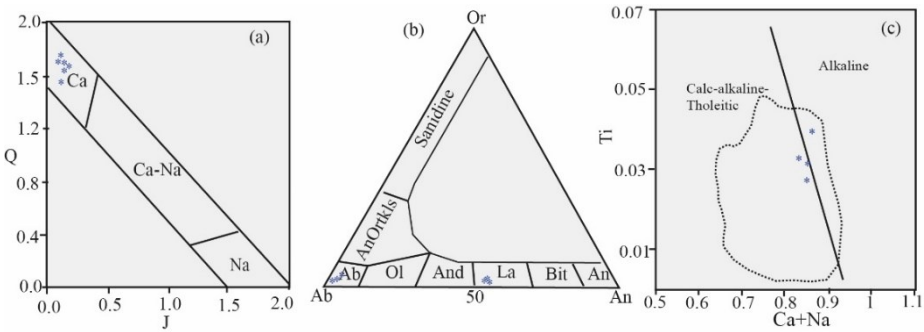

Şekil 12. *Mineral bileşimleri diyagramları. (a) Klinopiroksen mineralinin Q-J ikili diyagramı, (b) Klinopiroksen Ti – Ca + Na dağılımı, (c) Plajiyoklasın Or-Ab-An üçgen diyagramı*

$NaAlSi_3O_8$ - $CaAl_2Si_2O_8$ bileşimine sahip plajiyoklazların analiz sonuçları Tablo 3'te verilmiştir. Seçilen plajiyoklazlar, %67-40 Anortit bileşimi ile andezin ve labradorit bileşimlidir. Tablo 2'de görüldüğü gibi, örneklerin Al_2O_3 içeriği %26.3-28.7, K_2O içeriği %0.65'tir. Sosüritleşme süreçlerinden etkilenen plajiyoklazlar, kalsiyum bakımından zengindir. Geç evrede hidrotermal sıvılar, sodyumca zengin plajiyoklazların gelişmesine sebep olmuştur (Kılıç ve Güler, 2023). Dolayısıyla, geç evre magmatik ve metasomatik süreçlerde, Ca-zengin plajiyoklazlar Na-zengin plajiyoklazlara dönüşmektedir. Bu nedenle, Ca-plajiyoklazın geç evre dönüşümü albite-oligoklaz oluşumuna yol açmıştır.

4. Sonuçlar

Burdur İli'nin 70 km güneybatısında, Yeşilova İlçesi, Ulupınar ve İğdir köyleri arasındaki Yeşilova ofiyoliti gabro birimlerinin petrografisi ve mineral kimyasını incelemeyi amaçlayan bu çalışma, yaklaşık 35km²' lik bir alanı kapsar. Bu alan, 1/25.000 ölçekli Denizli $M_{23}b_3$ ve $M_{23}c_2$ haritaları içerisinde bulunur.

Yeşilova Ofiyoliti, altındaki Kızılcadağ melanjı ve metamorfitlerin bulunduğu alanda, farklı amaçlı birçok çalışma yapılmıştır (Özpınar & ark., 1996; Kılıç, 2012). Güncel çalışmalardan biri, iğdir

metamorfitlerinin adayayı toleyit bileşimine sahip amfibolitlerinde yapılan $\delta_{18}O$ izotop analizidir (Kılıç, 2012). Araştırmacı, İğdır metamorfiti garnet amfibolitlerinin $\delta_{18}O$ 'nın %4.2 belirlemiş ve amfibolitlerin magmatik bir kökene sahip olduğunu ifade etmiştir. Bir diğer çalışma Aslan (2023) tarafından İğdir metamorfiti üzerine yapılan çalışmadır. Araştırmacı, Burdur ve çevresini kapasayan çalışmasında Yeşilova ofiyoliti tabanında yeralan metamorfitleri litolojik seviyelere ayırmış ve ayrıntılı jeolojik haritasını çıkartmıştır. Bu çalışmada metamorfitlerin, amfibolit fasiyesinden granülüt fasiyesine kadar değişen mineral parajenezi gösterdiğini ve metamorfitlerin ters metamorfizma özelliğine sahip olduğunu ifade etmiştir.

Likya Peridotitlerinin kökeni üzerine yapılan çalışmalarda (Özpınar& ark., 1996), farklı derecelerde tüketilmiş okyanus ortası sırtı ve supra-subduksiyon zonu kalıntı manto olduğu ifade edilmiştir. Karbonat platformu, Likya Ofiyoliti ve Kızılcadağ melanjı, Anadolu-Taurid karbonat platformunun pasif kıtasal kenar sedimentleri üzerine ilerlemesi ve tektonik sıkışma nedeniyle iç kesimlerde tamamen yok olmuştur. Her birim kendi içinde tektonizma etkisiyle farklı metamorfizma dereelerine sahiptir (Konak& ark.,2005). Neotetis Okyanusu'nun kuzey kolunun kapanması nedeniyle Anadolu-Taurid ile Pontidler arasında gerçekleşen kıta-kıta çarpışması, güney yönünde Likya naplarının ilerlemesine ve karbonat platformunun bükülmesiyle kıtaönü havzaya yerleşmesine sebep olmuştur. Likya Napları'nın güneydoğuya doğru en son Tortoniyen (Üst Miyosen) döneminde gerçekleşmiştir.

Eksik dizi özelliğindeki Yeşilova ofiyoliti, tabanda İğdır metamorfikleri, tavanda Kızılcadağ ofiyolit melanjıyla dokanak oluşturur. Kızılcadağ ofiyolit melanjı, kırmızı renkli kireçtaşı, radyolarit, serpantinit ve ultramafik kayaçlar matriks içinde dağınık şekilde görülmektedir. Kırmızımsı kahve renge sahip bu birim, çeşitli boyutlarda kayaç parçaları içermektedir. Kızılcadağ ofiyolit melanjı, mafik ve ultramafik kayalar, kırmızı kireçtaşları ve radyolaritten ibarettir.

Çoklu iz element diyagramlarında, Rb, Ba, K, Sr ve Eu gibi büyük iyonik yarıçaplı litofil elementlerde (LIL) zenginleşme ve Ta, Nb gibi yüksek yerçekimi alanı (HFS) elementlerinde ise bir azalma görülür. Yeşilova ofiyolitine ait örnekler, toleyitik ve alkali magma karakterine sahip, supra-subduksiyon zonunu karakterize etmektedir. Jeokimyasal veriler aynı zamanda, ana magmanın bir asthenosferik manto kaynağından beslendiğini göstermektedir. Collins & Robertson (1999), Karaman (2000), Çelik & Delaloye (2002), dolerit dayklarının subofitik doku sergilediğini ve amfibol, piroksen, plajiyoklaz, epidot, klorit, ilmenit ve sfen bileşiminde olduklarını, nematoblastik dokulu amfibolitlerin ise, amfibol, kalıntı piroksen, plajiyoklaz, ilmenit ve sfen içerdiklerini belirlemişlerdir. Koralay ve Özpınar (2003), Yeşilova ofiyolit dizisinin en üstünde yer alan altere bazaltlarda kimyasal analiz yapmış ve bu bazaltların, 'düşük potasyumlu bazalt', 'okyanus ortası sırtı bazaltı' ve 'N-MORB tipi bazaltlar' karakterlerine sahip, tüketilmiş manto kaynağını göstermektedir. Çelik & Delaloye (2003), Likya Ofiyolitleri'ne ait metamorfik kayaçların kimyasal analiz sonucunun, okyanus ortası sırtı bazaltı (MORB), ada yayı toleyitleri (IAT) ve plaka içi bazalt alanına düştüğünü ve Antalya Ofiyoliti'ne ait metamorfik dilim kayaçlarının ise ada yayı toleyitleri (IAT) olduğunu belirlemişlerdir.

Likya, Antalya, Beyşehir, Mersin, Alihoca ve Pozantı-Karsantı ofiyolitlerinin metamorfik dilimlerindeki amfibollerin 90.7±0.5 - 93.8±1.7 my, muskovitlerin ise 91.2±2.3 - 93.6±0.8 my soğuma yaşları elde edilmiştir (Çelik & ark., 2006).

Kaynak:

Özcengiz, D. (2012). Yoğun bakımda sıvı tedavisi. *Yoğun Bakım Dergisi, 10* (1), 29-39.

Ersoy, Ş.,. Batı Toros (Likya) Napları'nın Yapısal Öğelerinin ve Evriminin Analizi, T.M.M.O.B., J.M.O., Jeoloji Mühendisliği Dergisi 1990;37:5-16.

[3] Ketin, İ., Tectonic units of Anatolia (Asia Minor). Min. Res. Expl. Inst. Turkey 1966; 66: 23-34.

[4] Şengör, A.M.C. ve Yılmaz, Y.,. Tethyan evolution of Turkey: a plate tectonic approach. Tectonophysics, 1981;75:181-241.

[5] Okay, A. İ., Tansel, İ. ve Tüysüz, O. Obduction, subduction and collision as reflected in the Upper Cretaceous-Lower Eocene sedimentary record of western Turkey: Geological Magazine 2001; 138/2: 117–142.

[6] Candan, O., Dora, O.Ö., Oberhanslı, R., Koralay, E., Çetinkaplan, M., Akal C., Satır, M., Chen, F. ve Kaya, O., Stratigraphy of the Pan-African basement of the Menderes Massif and the realationship with Late NeoProterozoic/Cambrien evolution of the Gondwana. MTA Bülteni, 2011;141:25-68.

[7] Karaman, M.E. Isparta-Burdur arasının jeolojisi ve tektonik özellikleri. Türkiye Jeoloji Kurumu Bülteni 1994; 37(2): 119-134.

[8] Şenel, M., , Selçuk, H., Bilgin, Z.R., Şen, M.A., Karaman, T., Erkan, M., Kaymakçı, H., Örçen., S. ve Bilgi, C., Likya napları ön cephe özellikleri (GB Türkiye). TJK Bildiri Özleri, 1987; 6.

[12] Burns, L.E., The Border Ranges Ultramafic and Mafic Complex, South Central Alaska: Cumulate Fractionates of Island Arc Volcanics. Canadian Journal of Earth Sciences 1985; 22:1020-1038.

[13] Aksoy, R. ve Aksarı, S. Elmalı (Antalya, Batı Toroslar) kuzeyinde Likya Naplarının Jeolojisi", J. Fac. Eng. Arch. Selcuk Univ., 2008;23:2, 45-57.

[14] Karaman, T. Yeşilova-Tefenni (Burdur) Batısında Kalan Alanın Jeolojisi ve Petrografisi, Yüksek Lisans Tezi, 84s., S.Ü. Fen Bilimleri Enstitüsü, 1987; Konya.

[16] Kılıç, A.D., Iğdir (Acıgöl-Burdur) Civarının Jeolojik ve Petrografik Açıdan İncelenmesi, Pamukkale Üniversitesi Yüksek Lisans Tezi, 1996, 65s.

[19] Stoneley, R., On the Origin of Ophiolite Complexes in the Southeastern Tethyan Region. Tectonophysics 1975; 75: 181-241.

[20] Bernouilli, D., Graciansky, P.C. ve Monod, O. The extension of the Lycian nappes (SW Turkey) into the Southeastern Aegean island. Eclogae geol. Helv., 1974; 67- 4-90.

[21] Çelik, Ö.F. ve Chiaradia, M., Geochemical and petrological aspects of dike intrusions in the Lycian ophiolites (SW Turkey): a case study for the dike emplacement along the Tauride Belt Ophiolites, Int. J. Earth Sci. (Geol. Rundsch), 2008;97:1151–1164.

[23] Dora, Ö.O., Candan, O., Dürr, St. ve Oberhansli, R. New evidence on the geotectonic evolution of the Menderes massif. I.E.S.C.A. Proceedings 1995; 1: 53-72.

[24] Gessner, K., Piazolo, S., Güngör, T., Ring, U., Kröner, A. ve Passchier, C.W. Tectonic significance of deformation in granitoid rocks of the Menderes nappes, Anatolide belt, southwest Turkey. International Journal of Earth Sciences 2001; 89: 766-780.

[26] Thuizat, R., Whitechurch, H., Montigny, R., ve Juteau, T. K-Ar dating of some infra-ophiolitic metamorphic soles from the eastern Mediterranean: New evidence for oceanic thrusting before obduction. Earth and Planetary Science Letters 1981; 52: 302-310.

[27] Erakman, B., Meşhur, M., Gül, M., Alkan, H., Öztaş, Y. ve Akpınar, M. Fethiye-Köyceğiz-TefenniElmalı-Kalkan arasında kalan alanın jeolojisi, Türkiye, 6. Petrol Kongresi, Ankara, 1982: 23-31.

[28] Koçyiğit, A. Isparta Büklümünde (Batı Toroslar) Toroslar Karbonat Platformunun Jeolojik Evrimi. Türkiye Jeoloji Kurultayı Bülteni, 1981; 24: 2,15-23.

[34] Irvine, T.N., & Baragar, W.R.A. (1971). A guide to the chemical classification of the common volcanic rocks. Canadian Journal of Earth Sciences, 8(5), 523-548. http://doi.org/10.1139/e71-055

[35] Zhang, J.H., Ge, W.C., Wu, F.Y., Wilde, S.A., Yang, J.H., Liu, X.M. Large-scale Early Cretaceous volcanic events in the northern Great Xing'an Range, NortheasternChina. Lithos, 2008b;102:138–157.

[40] Gao, S., Luo, T.C., Zhang, B.R., Zhang, H.F., Han, Y.W., Hu, Y.K., Zhao, Z.D., Chemical composition of the continental crust as revealed by studies in East China. Geochimica et Cosmochimica Acta ;1998a: 62, 1959–1975.

[41] A. K. Middlemost. Magmas and Magmatic Rocks. An Introduction to Igneous Petrology. x + 266 pp. London, New York: Longman. Price £13.95 (paperback). ISBN 0 582 30080 0. Geological Magazine. 1986;123(1):87-88. doi:10.1017/S0016756800026716

[42] Pearce J.A.Trace element characteristics of lavas from destructive plate boundaries In : Thorpe RS (ed) Orogenic andesites. J Wiley and Sons, 1982: 525-548.

[43] Sun SS, Nesbitt RW, Sharaskin AY (1979) Geochel~aical characteristics of mid-ocean ridge basalts. Earth Planet Sci Lett1979; 44:119-138

[44] Boynton, V. Cosmochemistry of the rare earth elements: meteorite studies, in rare earth element geochemistry. Ed. by P. Henderson Elsevier Amsterdam, 1984: 63–114.

[46] Döyen A., Çömlekçiler F. ve Koçak K. Stratigraphic Features of the Yeşilova Ophiolite, Burdur, South-Western Turkey, Springer Geology, Strati 2013: 493-498.

[47] Kılıç, A.D. Petrogenesis of Subduction Zone and Dunite Bodies. Journal of Earth Science and Engineering, 2012; 2(7): 377-386.

[48] Özpınar, Y., Tayfun, E. ve Kılıç, A.D. Salda Gölü (Yeşilova-Burdur) Çevresindeki Ofiyolitlerin Petrografisi ve Salda Gölü Manyezit Oluşumlarının Jeokimyasal İncelemesi, Çukurova Üniversitesi Yerbilimleri Dergisi, 1996; 28: 125-142.

Kocak, K., Isik, F., Arslan, M., and Zedef, V., 2005,Petrological and source region characteristics of ophiolitic hornblende gabbros from the Aksaray and Kayseri regions, Central Anatolian Crystalline Complex, Turkey: Journal of Asian Earth Sciences, v.25, p. 883–891.

Kılıç, A.D., Karaca, T. 2021. Fay Kayalarının Mineralojisinde Deformasyonun Rolü. European Journal of Science and Technology 27, 942-949

AD KILIÇ, 2017. Microstructure and Mineralogic Evidences of Fractional Differentiation: The Yeşilova Ophiolite Example, Journal of Earth Science and Engineering 7, 23-26.

AD Kılıç, M Güler, 2023. Metamorfik Masiflerin Asitik Bileşenleri: Jeokimya ve Mineraloji Perspektifi,Avrupa Bilim ve Teknoloji Dergisi, 71-79

BIDCE